111-27-CR
135334
p. 43

NASA
Technical
Memorandum

NASA TM - 108386

(NASA-TM-108386) THE EFFECT OF TENSILE STRESS ON HYDROGEN DIFFUSION IN METAL ALLOYS (NASA) 43 p

N93-16701

Unclas

G3/26 0135334

THE EFFECT OF TENSILE STRESS ON HYDROGEN DIFFUSION IN METAL ALLOYS

By M.D. Danford

Materials and Processes Laboratory
Science and Engineering Directorate

December 1992

National Aeronautics and
Space Administration

George C. Marshall Space Flight Center

REPORT DOCUMENTATION PAGE

Form Approved
OMB No. 0704-0188

Public reporting burden for this collection of information is estimated to average 1 hour per response, including the time for reviewing instructions, searching existing data sources, gathering and maintaining the data needed, and completing and reviewing the collection of information. Send comments regarding this burden estimate or any other aspect of this collection of information, including suggestions for reducing this burden, to Washington Headquarters Services, Directorate for Information Operations and Reports, 1215 Jefferson Davis Highway, Suite 1204, Arlington, VA 22202-4302, and to the Office of Management and Budget, Paperwork Reduction Project (0704-0188), Washington, DC 20503.

1. AGENCY USE ONLY (Leave blank)	2. REPORT DATE	3. REPORT TYPE AND DATES COVERED
	December 1992	Technical Memorandum

4. TITLE AND SUBTITLE

The Effect of Tensile Stress on Hydrogen Diffusion in Metal Alloys

5. FUNDING NUMBERS

6. AUTHOR(S)

M.D. Danford

7. PERFORMING ORGANIZATION NAME(S) AND ADDRESS(ES)

George C. Marshall Space Flight Center
Marshall Space Flight Center, Alabama 35812

8. PERFORMING ORGANIZATION REPORT NUMBER

9. SPONSORING/MONITORING AGENCY NAME(S) AND ADDRESS(ES)

National Aeronautics and Space Administration
Washington, DC 20546

10. SPONSORING/MONITORING AGENCY REPORT NUMBER

NASA TM - 108386

11. SUPPLEMENTARY NOTES

Prepared by Materials and Processes Laboratory, Science and Engineering Directorate.

12a. DISTRIBUTION/AVAILABILITY STATEMENT

Unclassified — Unlimited

12b. DISTRIBUTION CODE

13. ABSTRACT *(Maximum 200 words)*

The effect of tensile stress on hydrogen diffusion has been determined for Type 303 stainless steel, A286 CRES, and Waspaloy and IN100 nickel-base alloys. It was found that hydrogen diffusion coefficients are not significantly affected by stress, while the hydrogen permeabilities are greatly affected in Type 303 stainless steel and A286 CRES (iron-based alloys), but are affected little in Waspaloy (nickel-base) and not affected at all in IN100 (nickel base). These observations might be taken as an indication that hydrogen permeabilities are affected by stress in iron-based alloys, but only slightly affected in nickel-based alloys. However, it is too early to make such a generalization based on the study of only these four alloys.

14. SUBJECT TERMS

Hydrogen diffusion in metals, hydrogen diffusion coefficients and stress, hydrogen diffusion and permeability with stress, hydrogen trapping and stress

15. NUMBER OF PAGES
44

16. PRICE CODE
NTIS

17. SECURITY CLASSIFICATION OF REPORT	18. SECURITY CLASSIFICATION OF THIS PAGE	19. SECURITY CLASSIFICATION OF ABSTRACT	20. LIMITATION OF ABSTRACT
Unclassified	Unclassified	Unclassified	Unlimited

TABLE OF CONTENTS

	Page
INTRODUCTION	1
EXPERIMENTAL	1
RESULTS	2
Type 303 Stainless Steel	2
A286 CRES	3
Waspaloy (Nickel-Base Alloy)	3
IN100 (Nickel-Base Alloy)	3
DISCUSSION AND CONCLUSIONS	4
REFERENCES	5

PRECEDING PAGE BLANK NOT FILMED

LIST OF ILLUSTRATIONS

Figure	Title	Page
1.	Hydrogen Desorption Curves for Type 303SS at Zero Stress	13
2.	Hydrogen Desorption Curves for Type 303SS at 25 Percent of Yield	14
3.	Hydrogen Desorption Curves for Type 303SS at 50 Percent of Yield	15
4.	Hydrogen Desorption Curves for Type 303SS at 75 Percent of Yield	16
5.	Hydrogen Desorption Curves for Type 303SS at 90 Percent of Yield	17
6.	Least-Squares Fit of a Second-Degree Polynomial to Percent Uniformity Versus Percent Yield for Type 303SS	18
7.	Hydrogen Desorption Curves for A286 CRES at Zero Stress	19
8.	Hydrogen Desorption Curves for A286 CRES at 25 Percent of Yield	20
9.	Hydrogen Desorption Curves for A286 CRES at 50 Percent of Yield	21
10.	Hydrogen Desorption Curves for A286 CRES at 75 Percent of Yield	22
11.	Hydrogen Desorption Curves for A286 CRES at 90 Percent of Yield	23
12.	Least-Squares Fit of a Second-Degree Polynomial to Percent Uniformity Versus Percent Yield for A286 CRES	24
13.	Hydrogen Desorption Curves for Waspaloy at Zero Stress	25
14.	Hydrogen Desorption Curves for Waspaloy at 25 Percent of Yield	26
15.	Hydrogen Desorption Curves for Waspaloy at 50 Percent of Yield	27
16.	Hydrogen Desorption Curves for Waspaloy at 75 Percent of Yield	28
17.	Hydrogen Desorption Curves for Waspaloy at 90 Percent of Yield	29
18.	Least-Squares Fit of a Second-Degree Polynomial to Percent Uniformity Versus Percent Yield of Waspaloy	30
19.	Hydrogen Desorption Curves for IN100 at Zero Stress	31
20.	Hydrogen Desorption Curves for IN100 at 25 Percent of Yield	32
21.	Hydrogen Desorption Curves for IN100 at 50 Percent of Yield	33

LIST OF ILLUSTRATIONS (Continued)

Figure	Title	Page
22.	Hydrogen Desorption Curves for IN100 at 75 Percent of Yield	34
23.	Hydrogen Desorption Curves for IN100 at 90 Percent of Yield	34

LIST OF TABLES

Table	Title	Page
1.	Chemical Analysis of Type 303 Stainless Steel Chips	6
2.	Parameters Obtained From 303SS Desorption Data	6
3.	Hydrogen Trapping by 303SS as a Function of Stress	7
4.	Chemical Analysis of A286 CRES	7
5.	Parameters Obtained From A286 CRES Desorption Data	8
6.	Hydrogen Trapping by A286 CRES as a Function of Stress	8
7.	Chemical Analysis of Waspaloy	9
8.	Parameters Obtained From Waspaloy Desorption Data	10
9.	Hydrogen Trapping by Waspaloy as a Function of Stress	10
10.	Chemical Analysis of IN100 Alloy	11
11.	Parameters Obtained From IN100 Desorption Data	12
12.	Hydrogen Trapping by IN100 as a Function of Stress	12

CHEMICAL SYMBOLS

Al	Aluminum
B	Boron
Bi	Bismuth
C	Carbon
Co	Cobalt
Cr	Chromium
Cu	Copper
Fe	Iron
Mo	Molybdenum
Mn	Manganese
Nb	Niobium
Ni	Nickel
O	Oxygen
P	Phosphorous
Pb	Lead
S	Sulfur
Si	Silicon
Ta	Tantalum
Ti	Titanium
V	Vanadium
W	Tungsten
Zr	Zirconium

TECHNICAL MEMORANDUM

THE EFFECT OF TENSILE STRESS ON HYDROGEN DIFFUSION IN METAL ALLOYS

INTRODUCTION

The present work was undertaken to provide further information regarding the effect of tensile stress on the hydrogen distribution in metals on charging and also on the effect on other parameters involved, such as mean hydrogen concentrations and hydrogen diffusion coefficients. Experimentally, it is desirable to carry out the investigations in the elastic region since determination of the hydrogen diffusion coefficient is a sensitive function of the sample radius, and deformation of the sample in the plastic region would prevent accurate determination of this parameter. However, small plastic deformations did occur at 90-percent yield, but these are not considered great enough to seriously affect the results.

Other studies concerning the influence of stress on hydrogen diffusion have been carried out. Wriedt and Oriani[1] showed that an elastically stressed 75-weight-percent palladium to 25-weight-percent silver alloy in a hydrogen atmosphere increased in hydrogen content under uniaxial tension and decreased in hydrogen content under uniaxial compression. Bockris et al.[2] studied Armco iron and 4340 steel and found that hydrogen permeation was increased by tensile stress and decreased by compressive stress, with the hydrogen diffusion coefficient being unaffected by the applied stress.

Results for A286 CRES steel have been reported previously.[3] The present study includes work on Type 303 stainless steel (303SS) and nickel-base alloys IN100 and Waspaloy. There are, therefore, two iron-base alloys and two nickel-base alloys, and it is of interest to compare the effect of stress on the hydrogen diffusion in these different alloys.

This report presents the results obtained by electrochemical methods on all four alloys under stresses corresponding to 0, 25, 50, 75, and 90 percent of yield. Calculations were made using the standard procedure previously developed and described[4] for data extending to large time (0 to 150,000 s).

EXPERIMENTAL

The EG&G-PARC model 350A corrosion measurement console was employed for the electrochemical measurements of hydrogen desorption.

Samples consisted of tensile specimens of the metal alloys which were 5.08-cm (2-in) long with a gauge length of 1.905 cm (0.75 in) and a diameter of 0.3175 cm (0.125 in). The specimens were threaded at both ends with 1/4-20 NC threads. All metal parts, except for the gauge section, were coated with Micromask stop-off lacquer to prevent electrical contact.

The specimens were mounted on a Korros Data slow strain rate (SSR) machine, enclosed in a glass cell having a 1-L capacity. The cell was filled with a 0.1N sodium hydroxide (NaOH) solution which provided a medium for charging of the sample with hydrogen and for conduction of the hydrogen

desorption current. The SSR machine was then driven to the proper load level, which was maintained throughout the charging and desorption stages. Sample blanks were run at a constant potential of 0.0 V versus the saturated calomel electrode. The period of measurement was 150,000 s for each sample with values of the current being recorded every 500 s. After running the blanks, the specimens were then electrolytically charged with hydrogen for a period of 1 h at a current density of 90 mA/cm^2.

Measurements of the desorption current were initiated immediately on completion of charging, with current measurements being taken in the same manner as for the blanks. After completion of each run, data were read to an IBM PC/AT computer for calculation purposes. Currents due only to hydrogen were obtained by subtraction of the currents for blanks. After data for both the hydrogen-containing sample and its blank were obtained, the experimental curve $Q(t)$, the coulombs of hydrogen desorbed after time t, versus time was obtained through integration of the current-time curves. Values of $Q(t)$ were corrected for cutoff at finite time (150,000 s) by procedures described previously,[4] obtaining values for Q^{∞}_{HM}, the observed concentration $\bar{C}$, the apparent surface concentration C_o, and the hydrogen-diffusion coefficient D. The procedures for obtaining these quantities are described in Reference 4. Theoretical hydrogen-desorption curves were calculated for both uniform and nonuniform hydrogen distributions using the computer program PDEONE.[5]

Residual hydrogen concentrations (hydrogen remaining after complete desorption of the mobile hydrogen) were determined using the Leco Model RH2 hydrogen analyzer. Calibration of the hydrogen analyzer was accomplished using standard samples. The gauge sections of the tensile test specimens were retained for these analyses after removing the remaining shoulders and threaded sections at each end with a diamond saw.

RESULTS

Type 303 Stainless Steel

The material used in this investigation had an ultimate tensile strength (UTS) of 589 MPa (85.4 ksi) and a yield strength (YS) of 265 MPa (38.4 ksi). The chemistry of the Type 303SS alloy is presented in Table 1. Hydrogen desorption curves, experimental and theoretical, are shown in Figures 1 through 5. Results were obtained under stresses of 0, 66.2 MPa (9.6 ksi), 132.3 MPa (19.2 ksi), 198.5 MPa (28.8 ksi), and 238.5 MPa (34.6 ksi). These stress levels represent 0, 25, 50, 75, and 90 percent of the yield strength, respectively.

Results from the data analyses are presented in Table 2. These indicate that there is no significant trend in the values of the diffusion coefficients at the various stress levels. Values of C_o, the apparent concentration of hydrogen at the sample surface, $\bar{C}$, the mean mobile hydrogen concentration in the sample, and the percent uniformity of the initial hydrogen concentration on charging (parameters related to hydrogen solubility) indicate that the permeability of Type 303SS increases with stress up to about 50 percent of yield and decreases thereafter. The curve relating the variation of percent uniformity with percent yield is shown in Figure 6, the data points being fitted with a second-degree polynomial.

Hydrogen trapping as a function of stress is shown in Table 3. The percent of trapped or residual hydrogen is quite high in all cases, the average percent residual hydrogen being 62.3 percent. The reason for the very high percentage of trapped hydrogen is not known, but may be due to the high weight percent of sulfur (0.25 percent) present in this alloy. Magnified photographs of the metal matrix show that

there are numerous stringers interspersed throughout, which are probably filled with sulfur or metallic sulfides. The hydrogen may be trapped in these regions either by the sulfur-containing materials or as molecular hydrogen.

A286 CRES

A286 CRES had a chemistry (Table 4) conforming to AMS 5732, but the UTS of 1,210 MPa (175.6 ksi) and a YS of 933 MPa (135.3 ksi) indicated that the material had been solution treated, cold worked, and precipitation heat treated. Hydrogen desorption curves are shown in Figures 7 through 11. Results were obtained under stresses of 0, 233 MPa (33.9 ksi), 467 MPa (67.7 ksi), 700 MPa (101.6 ksi), and 840 MPa (121.9 ksi), representing 0, 25, 50, 75, and 90 percent of the YS.

Results from the data analyses are presented in Table 5. Again, no significant trend in values of the diffusion coefficients is noted. Values of C_o, $\bar{C}$, and the percent uniformity of the initial hydrogen concentration on charging indicate that the permeability of A286 CRES increases up to about 60 percent of the yield strength, decreasing thereafter. The curve relating the variation of percent uniformity with percent yield is shown in Figure 12. Again, the data points were fitted with a second-degree polynomial.

The hydrogen trapping as a function of stress is shown in Table 5. The average percent of trapped hydrogen is 7.6 percent, much lower than that for Type 303SS.

Waspaloy

The Waspaloy material had a UTS of 1,392 MPa (202 ksi) and a YS of 1,024 MPa (148.6 ksi). The chemistry of Waspaloy is shown in Table 7. Hydrogen desorption curves are shown in Figures 13 through 17. Results were obtained under stresses of 0, 256 MPa (37.2 ksi), 512 MPa (74.3 ksi), 768 MPa (111.4 ksi), and 922 MPa (133.7 ksi), representing 0, 25, 50, 75, and 90 percent of the YS.

Results from the data analyses are presented in Table 8. As with the previous cases, there is no significant trend in values of the diffusion coefficients. Values of C_o and $\bar{C}$ are generally higher for specimens under stress, although there is some scatter. Results for the percent uniformity show a much less pronounced trend with increasing stress than the two iron-based alloys previously discussed. Hence, the permeability of this alloy is much less affected by stress than are those for A286 CRES and 303SS. The curve relating the variation of percent uniformity with percent yield is shown in Figure 18, with all observed data points again being fitted with a second-degree polynomial.

The hydrogen trapping as a function of stress is shown in Table 9. The average percent trapped hydrogen is 20.6 percent.

IN100

The IN100 material obtained from a powder metallurgy isothermal forging, heat treated at Sintech, Inc., had a UTS of 1,606 MPa (233 ksi) and a YS of 1,160 MPa (168.3 ksi). The chemistry of this material is shown in Table 10. Hydrogen desorption curves are shown in Figures 19 through 23. Results were obtained under stresses of 0, 290 MPa (42 ksi), 580 MPa (84 ksi), 870 MPa (126 ksi), and 1,044 MPa (151 ksi). These stress levels represent 0, 25, 50, 75, and 90 percent of the YS, respectively.

Results from the data analyses are presented in Table 11. There is again no significant trend in the values of the diffusion coefficients. The results are somewhat surprising, since it is obvious that IN100 shows no effects due to stress. The values of $\bar{C}$ appear to actually decrease with increasing stress, although this is probably attributable mostly to scatter in the experimental results. The percent uniformity remains 100-percent nonuniform throughout, indicating no increase in permeability. This is to be compared with the results obtained for A286 CRES, Type 303SS, and Waspaloy. A286 CRES and Type 303SS, both iron-based alloys, show the most pronounced changes in permeability with stress, while Waspaloy, a nickel-based alloy, is only slightly affected.

Hydrogen trapping as a function of stress is shown in Table 12. The average percent trapped hydrogen is 21.5 percent, comparable to the value obtained for Waspaloy (20.6 percent). Thus, the value of 62.3 percent obtained for Type 303SS is far higher than the values obtained for the other three alloys.

DISCUSSION AND CONCLUSIONS

The results all show no significant trends in values of the hydrogen diffusion coefficients, in agreement with the results of Bockris et al.[2] Distinct increases in the mean mobile hydrogen concentrations were observed at higher stress levels for Type 303SS, A286 CRES, and slightly in Waspaloy, but not observed for IN100, where there was no effect due to stress.

Since the values of the diffusion coefficients were nearly the same for all four metal alloys, the increased hydrogen penetration in type 303SS, A286 CRES, and Waspaloy on charging cannot be explained using standard diffusion theory along with the observed hydrogen diffusion coefficients, which were obtained in hydrogen desorption measurements. It is likely that the increased penetration is due to increased permeability. For a thin membrane, the permeability is given by

$$\text{Permeation} = \frac{DSP}{L} \quad . \tag{1}$$

Here, D is the hydrogen diffusion coefficient, S is the solubility of hydrogen, P is the exterior hydrogen pressure, and L is the membrane thickness. Percent uniformities of the hydrogen distributions are accompanied by factors related to the solubility of hydrogen in the metals, namely the mean mobile hydrogen concentrations $\bar{C}$.

The difference between the permeability of hydrogen in iron-base alloys and that in the nickel-base alloys has not previously been observed. From this limited work, it is too early to make a generalization that all iron-base and nickel-base alloys are affected differently by tensile stress, the iron-base alloys being much more affected than the nickel-base alloys. However, the observations made in this work might be an indication that this could be the case.

REFERENCES

1. Wriedt, H.A., and Oriani, R.A.: Acta Metall., vol. 18, 1970, p. 753.

2. Bockris, J. O'M., Beck, W., Genshawl, M.A., Subramanyan, P.K., and Williams, F.S.: Acta Metall., vol. 19, 1971, p. 1209.

3. Danford, M.D.: NASA Technical Memorandum TM-103537, May 1991.

4. Danford, M.D.: NASA Technical Paper 2744, July 1987.

5. Sincovec, R.F., and Madsen, N.K.: ACM Trans. Math. Software, vol. 1, 1975, pp. 232–260.

Table 1.
Chemical Analysis of Type 303 Stainless Steel Chips.

Element	MSFC Analysis Weight Percent	AMS 5640P, Type 1 Weight Percent
Cr	18.30	17.00 – 19.00
Ni	8.82	8.00 – 10.00
Si	0.31	1.00 Maximum
Mn	1.70	2.00 Maximum
Mo	0.18	0.75 Maximum
Cu	0.56	0.75 Maximum
P	0.03	0.15 Maximum
Fe	Balance	Balance
C	0.087	0.15 Maximum
S	0.254	0.15 Minimum

Table 2.
Parameters Obtained from 303SS Desorption Data.

Percent Yield	$D \times 10^8$ cm^2/s	C_o*	$\bar{C}$†	Percent Uniformity
0	6.18	10.87	2.27	0
25	6.86	22.60	4.94	41.0
50	4.83	23.89	4.48	35.0
75	2.26	34.32	4.76	12.0
90	3.62	24.93	4.14	16.0

* Apparent H concentration at sample surface.
† Mean H concentration.

Table 3.
Hydrogen Trapping by 303SS as a Function of Stress.

Percent Yield	Mobile Hydrogen (p/m)	Trapped Hydrogen (p/m)	Total Hydrogen (p/m)	Percent Trapped Hydrogen
0	2.27	7.92	10.19	77.7
25	4.94	9.93	14.87	66.8
50	4.48	5.68	10.16	55.9
75	4.76	5.46	10.22	53.4
90	4.14	5.60	9.74	57.5

Table 4.
Chemical Analysis of A286 CRES.

Elements	MSFC Analysis Weight Percent	AMS 5732 Weight Percent
Cu	0.08	–
V	0.28	0.10 – 0.50
Si	0.25	1.0 Maximum
B	0.007	0.003 – 0.10
Al	0.27	0.35 Maximum
Ti	2.24	1.90 – 2.35
Mo	1.09	1.00 – 1.50
Mn	0.19	2.0 Maximum
Fe	57.33	Balance
Ni	24.43	24.0 – 27.0
Cr	13.77	13.5 – 16.0
P	0.014	0.25 Maximum
C	0.05	0.08 Maximum
S	0.001	0.025 Maximum

Table 5.
Parameters Obtained From A286 CRES Desorption Data.

Percent Yield	$D \times 10^8$ cm^2/s	C_o* (p/m)	$\bar{C}$ † (p/m)	Percent Uniformity
0	4.17	31.11	5.49	23
25	2.17	68.96	8.62	48
50	2.04	73.95	8.97	88
75	2.35	51.92	6.73	62
90	2.47	64.58	8.57	64

* Apparent H concentration at sample surface.
† Mean H concentration.

Table 6.
Hydrogen Trapping by A286 CRES as a Function of Stress.

Percent Yield	Mobile Hydrogen (p/m)	Trapped Hydrogen (p/m)	Total Hydrogen (p/m)	Percent Trapped Hydrogen
0	5.49	0.68	6.17	10.9
25	8.62	0.96	9.58	10.0
50	8.97	0.40	9.37	4.3
75	6.73	0.77	7.50	10.3
90	8.57	0.20	8.77	2.3

Table 7.
Chemical Analysis of Waspaloy.

Elements	MSFC Analysis Weight Percent	ASTM E354 Weight Percent
Cr	18.90	18.00 – 21.00
Co	12.80	12.00 – 15.00
C	0.060	0.02 – 0.10
Fe	0.56	2.0 Maximum
Mo	3.80	3.5 – 5.0
Ti	2.80	2.75 – 3.25
Al	1.40	1.2 – 1.6
Zr	0.063	0.02 – 0.08
B	0.0062	0.003 – 0.010
Mn	0.03	0.10 Maximum
Si	0.03	0.15 Maximum
Cu	Trace	0.10 Maximum
P	0.005	0.015 Maximum
Ni	Balance	Balance

Table 8.
Parameters Obtained From Waspaloy Desorption Data.

Percent Yield	$D \times 10^8$ cm^2/s	C_o* (p/m)	$\bar{C}$ † (p/m)	Percent Uniformity
0	5.18	26.13	5.08	0
25	5.40	31.19	6.17	9.7
50	5.79	21.30	4.35	14.2
75	3.92	32.35	5.58	11.9
90	5.02	33.73	6.47	17.4

* Apparent H concentration at sample surface.
† Mean H concentration.

Table 9.
Hydrogen Trapping by Waspaloy as a Function of Stress.

Percent Yield	Mobile Hydrogen (p/m)	Trapped Hydrogen (p/m)	Total Hydrogen (p/m)	Percent Trapped Hydrogen
0	5.08	2.41	7.49	32.2
25	6.17	1.26	7.43	17.0
50	4.35	1.29	5.64	22.9
75	5.58	1.53	7.11	21.5
90	6.47	0.66	7.13	9.3

Table 10.
Chemical Analysis of IN100 alloy.

Elements	MSFC Analysis Weight Percent	PWA 1074 Weight Percent
Ni	–	Balance
Co	18.74	18.0 – 19.0
Ti	4.38	4.15 – 4.50
Cr	12.39	11.90 – 12.90
Al	4.80	4.80 – 5.15
Mo	3.15	2.80 – 3.60
Bi	<0.001	0.00005 Maximum
Pb	<0.003	0.0002 Maximum
Cu	0.03	0.07 Maximum
Zr	0.06	0.04 – 0.08
W	0.01	0.05 Maximum
Nb+Ta	0.048	0.04 Maximum
Si	0.03	0.10 Maximum
Mn	<0.001	0.02 Maximum
Fe	0.15	0.30 Maximum
V	0.64	0.58 – 0.98
B	0.014	0.016 – 0.024
P	0.001	0.01 Maximum
C	0.0711	0.05 – 0.09
S	0.0007	0.01 Maximum
O	0.0168	0.010 Maximum

Table 11.
Parameters Obtained From IN100 Desorption Data.

Percent Yield	$D \times 10^8$ cm^2/s	C_o* (p/m)	$\bar{C}$ † (p/m)	Percent Uniformity
0	1.00	55.80	6.09	0
25	1.45	46.97	5.65	0
50	5.84	25.50	5.19	0
75	2.47	36.21	5.19	0
90	6.41	13.10	2.78	0

* Apparent H concentration at sample surface.
† Mean H concentration.

Table 12.
Hydrogen Trapping by IN100 as a Function of Stress.

Percent Yield	Mobile Hydrogen (p/m)	Trapped Hydrogen (p/m)	Total Hydrogen (p/m)	Percent Trapped Hydrogen
0	6.09	2.93	9.02	32.5
25	5.65	0.43	6.08	7.1
50	5.19	1.57	6.76	23.2
75	5.19	0.34	5.53	6.1
90	2.78	1.70	4.40	38.6

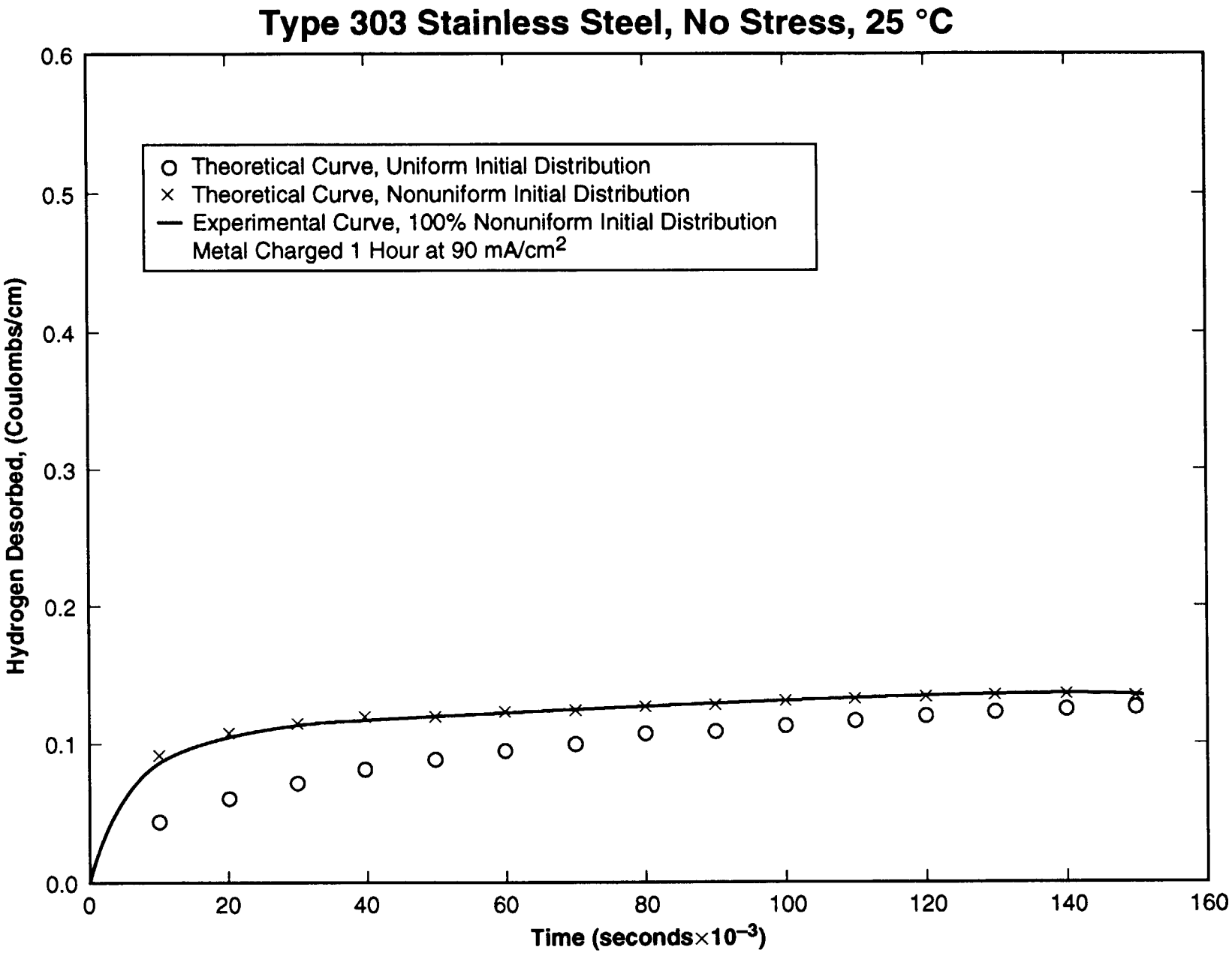

Figure 1. Hydrogen Desorption Curves for Type 303SS at Zero Stress.

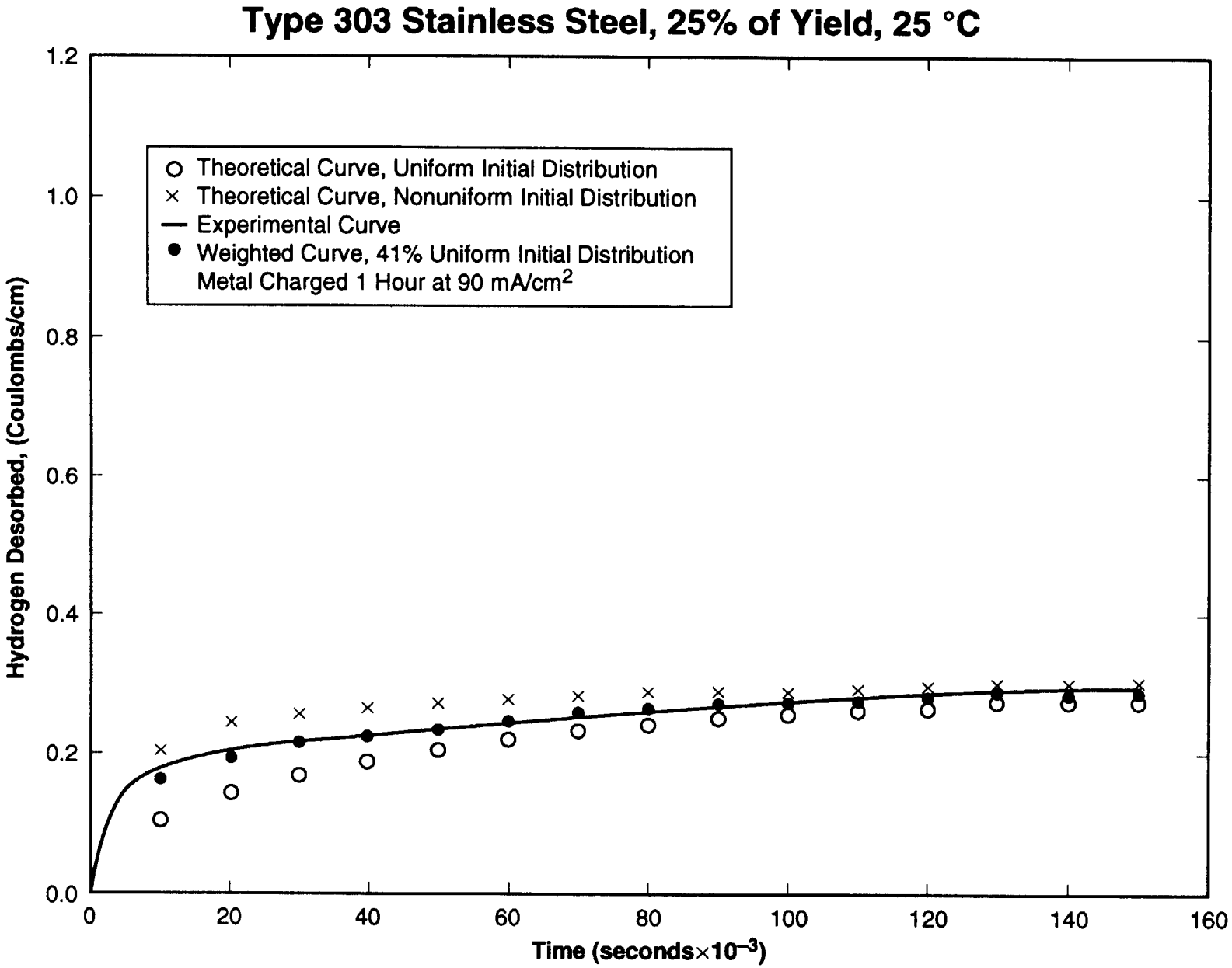

Figure 2. Hydrogen Desorption Curves for Type 303SS at 25 Percent of Yield.

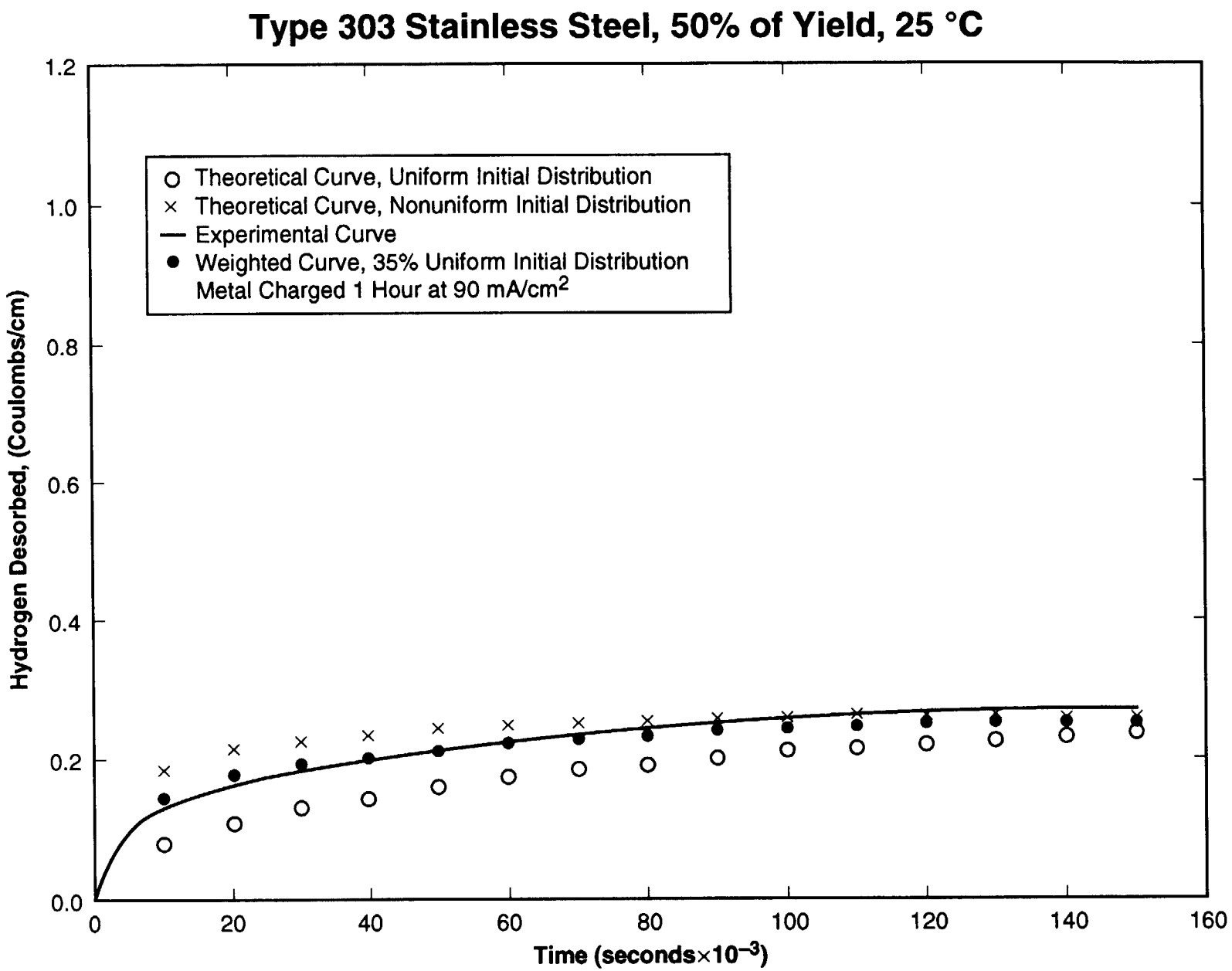

Figure 3. Hydrogen Desorption Curves for Type 303SS at 50 Percent of Yield.

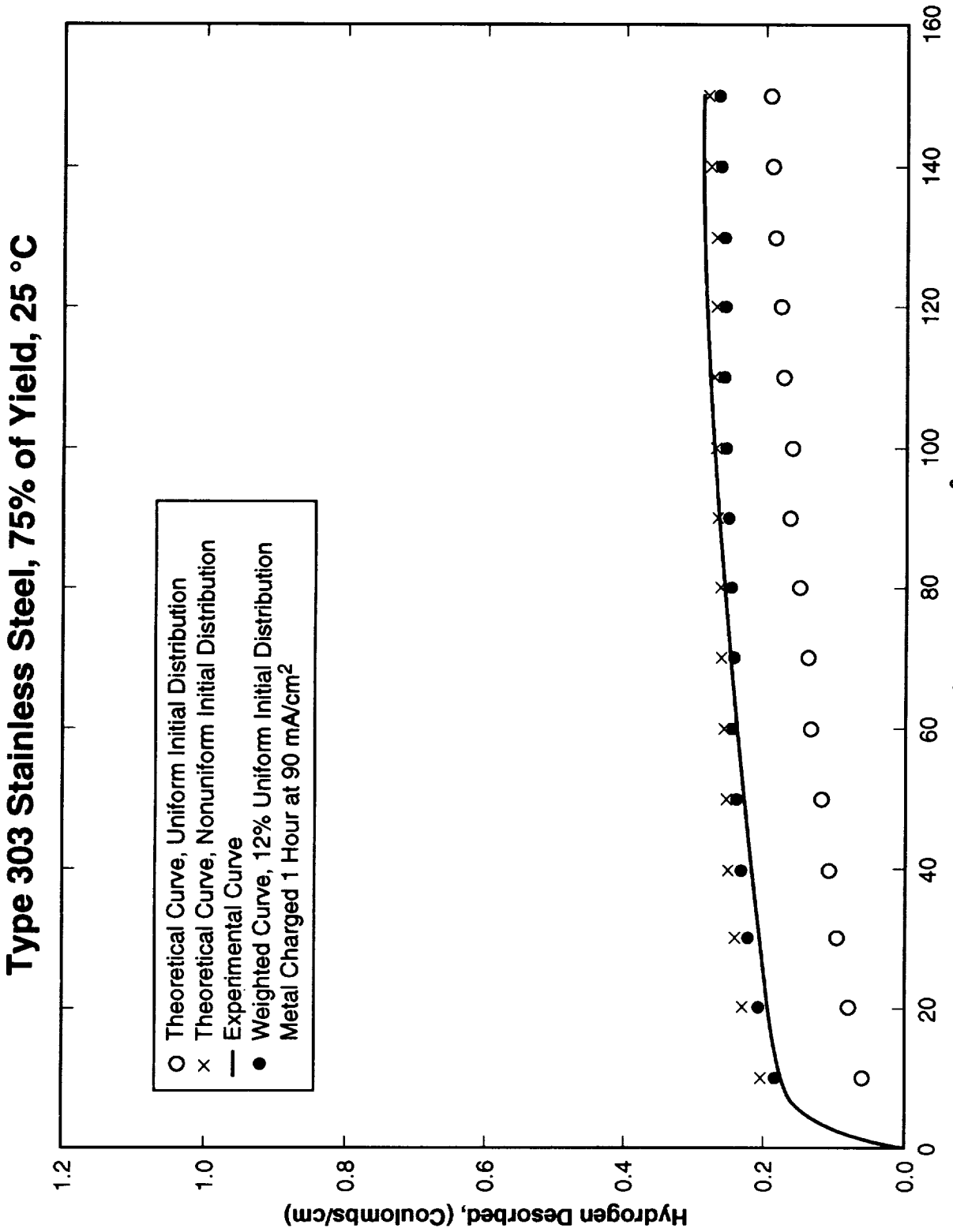

Figure 4. Hydrogen Desorption Curves for Type 303SS at 75 Percent of Yield.

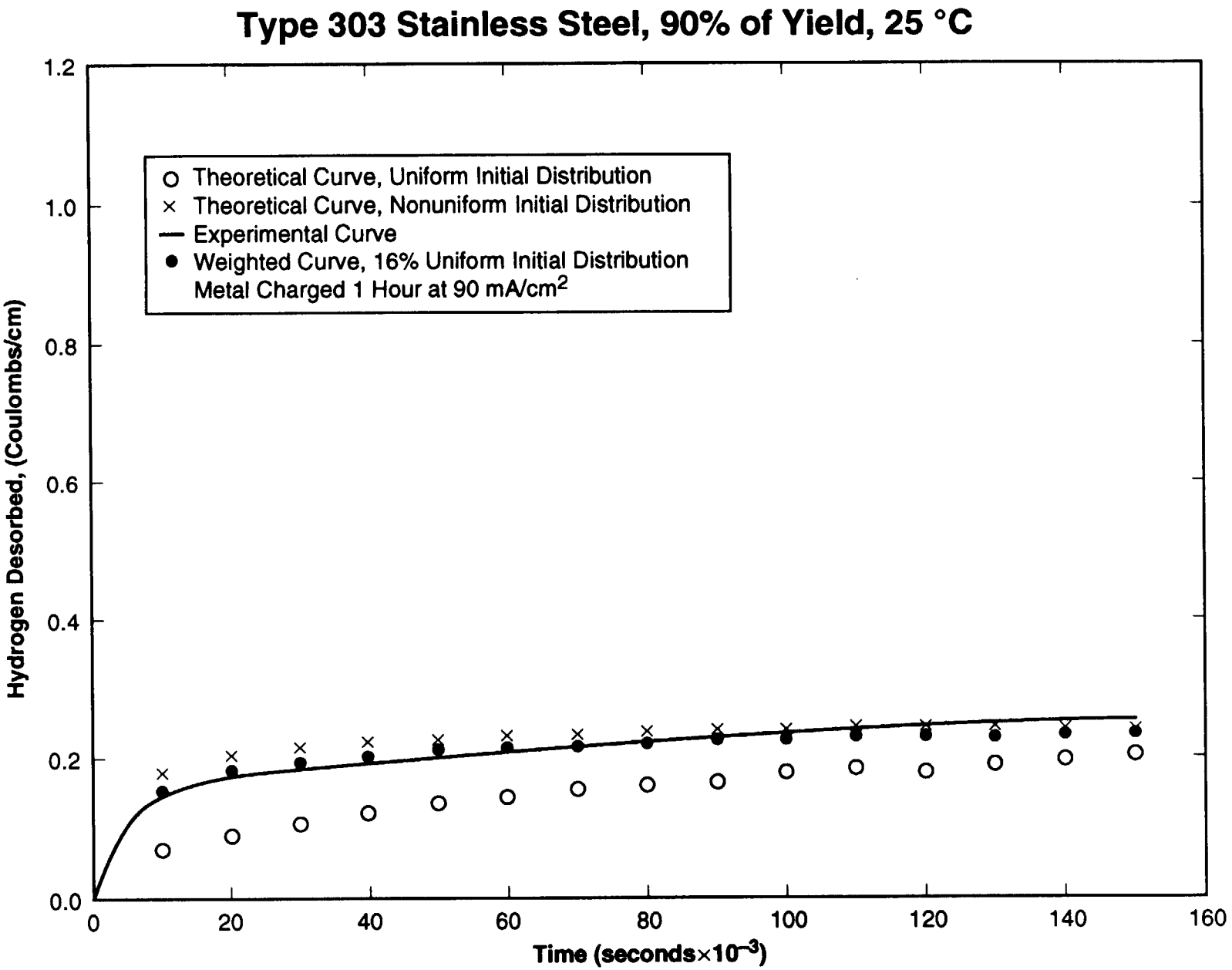

Figure 5. Hydrogen Desorption Curves for Type 303SS at 90 Percent of Yield.

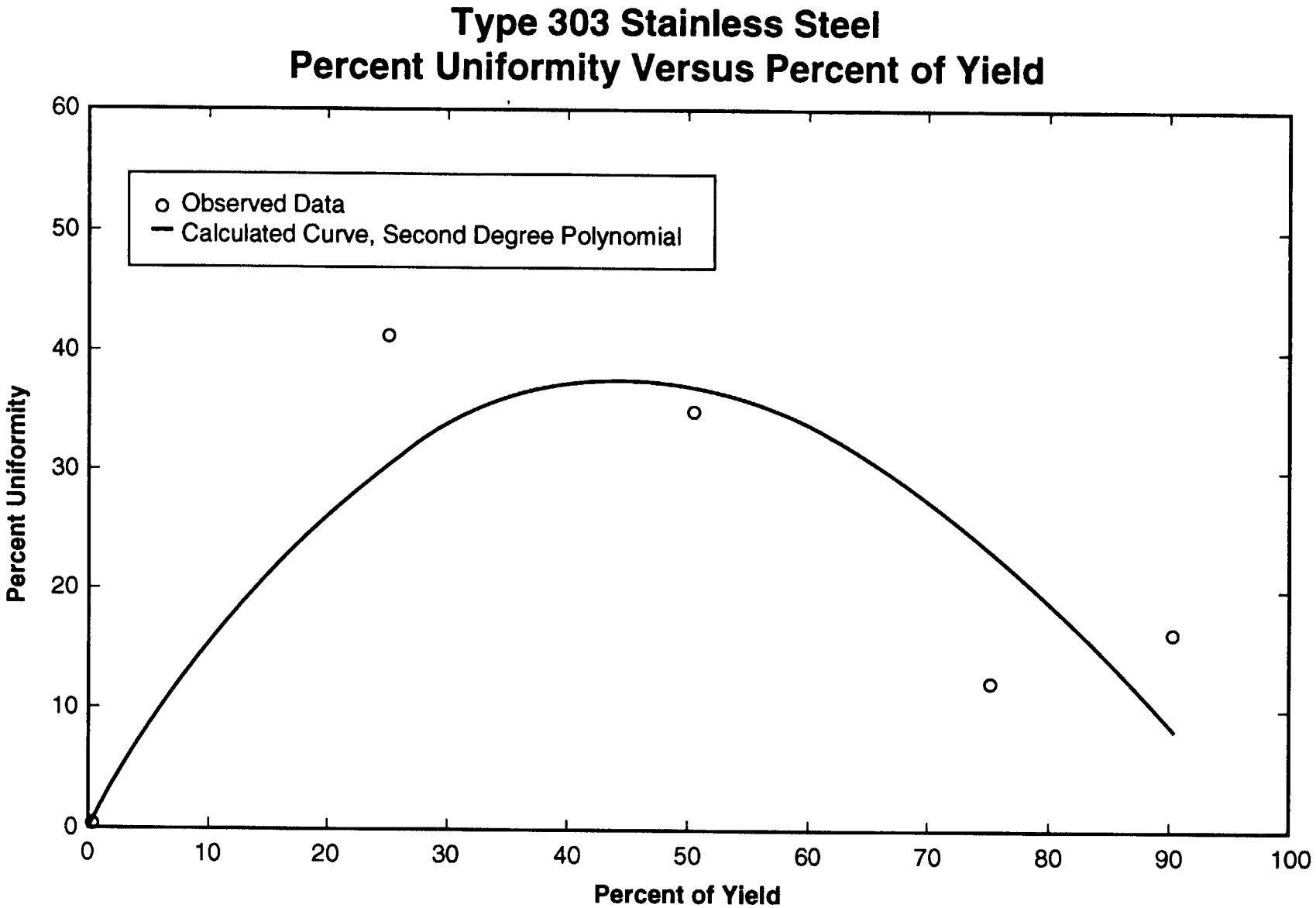

Figure 6. Least-Squares Fit of a Second-Degree Polynomial to Percent Uniformity Versus Percent Yield for Type 303SS.

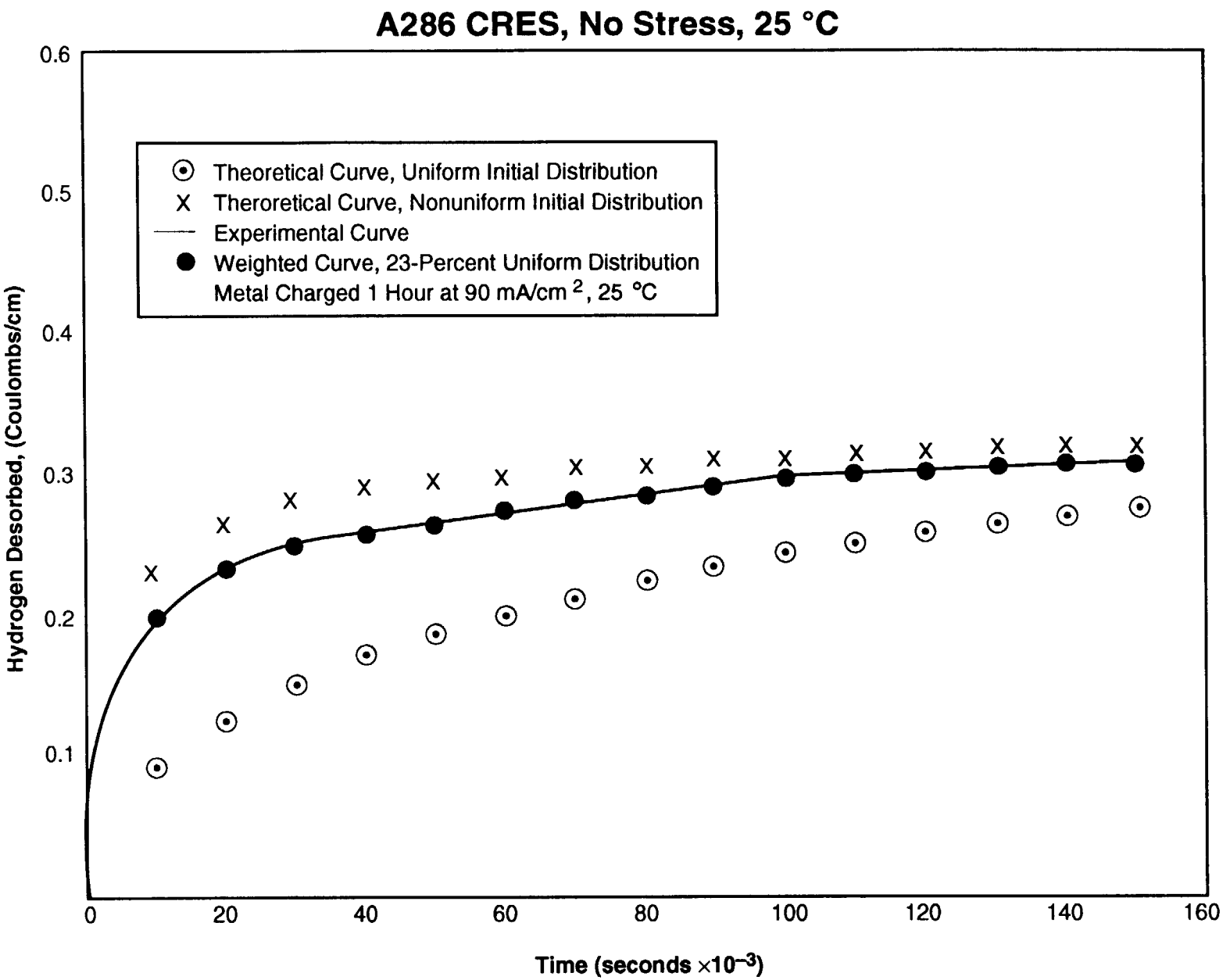

Figure 7. Hydrogen Desorption Curves for A286 CRES at Zero Stress.

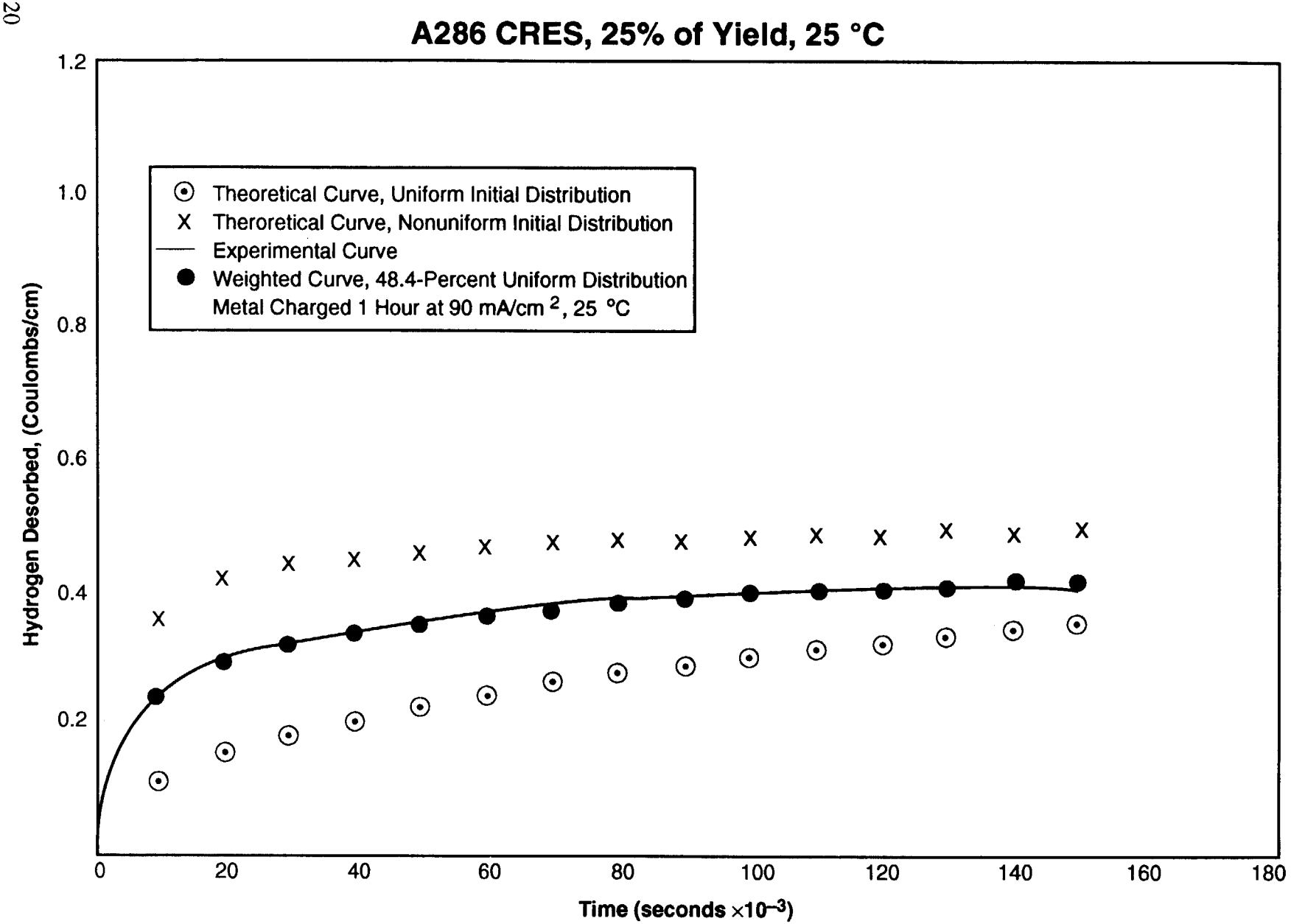

Figure 8. Hydrogen Desorption Curves for A286 CRES at 25 Percent of Yield.

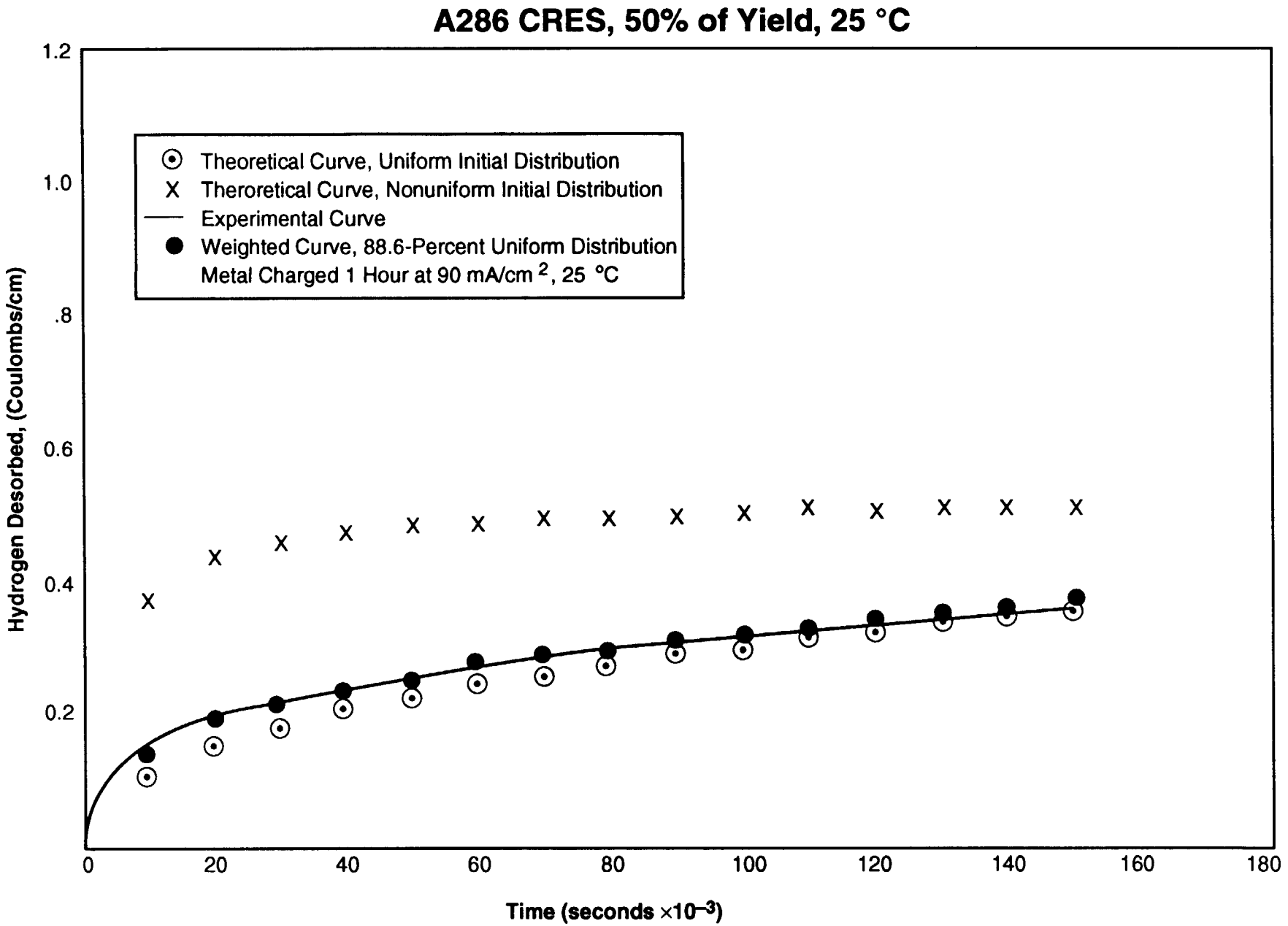

Figure 9. Hydrogen Desorption Curves for A286 CRES at 50 Percent of Yield.

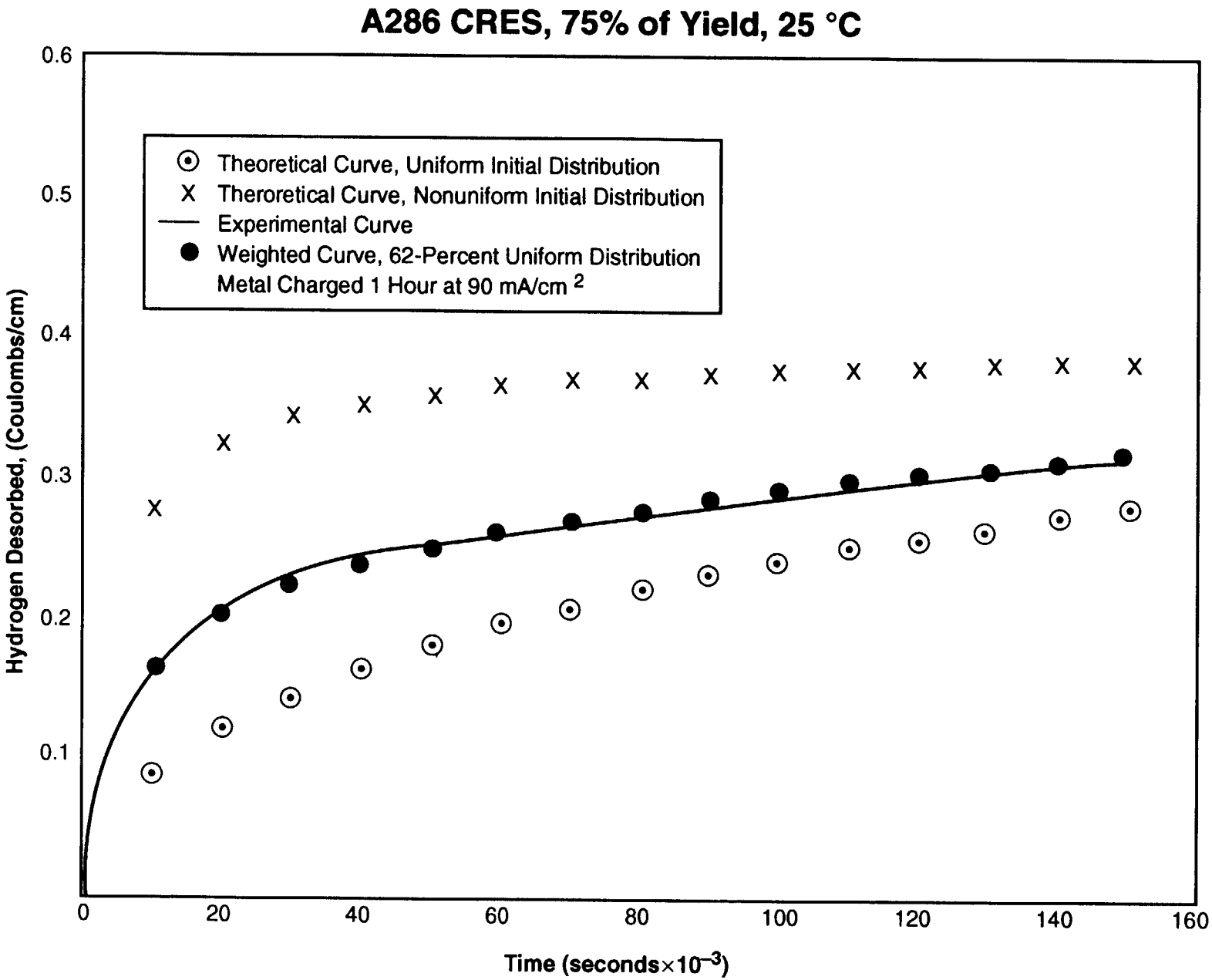

Figure 10. Hydrogen Desorption Curves for A286 CRES at 75 Percent of Yield.

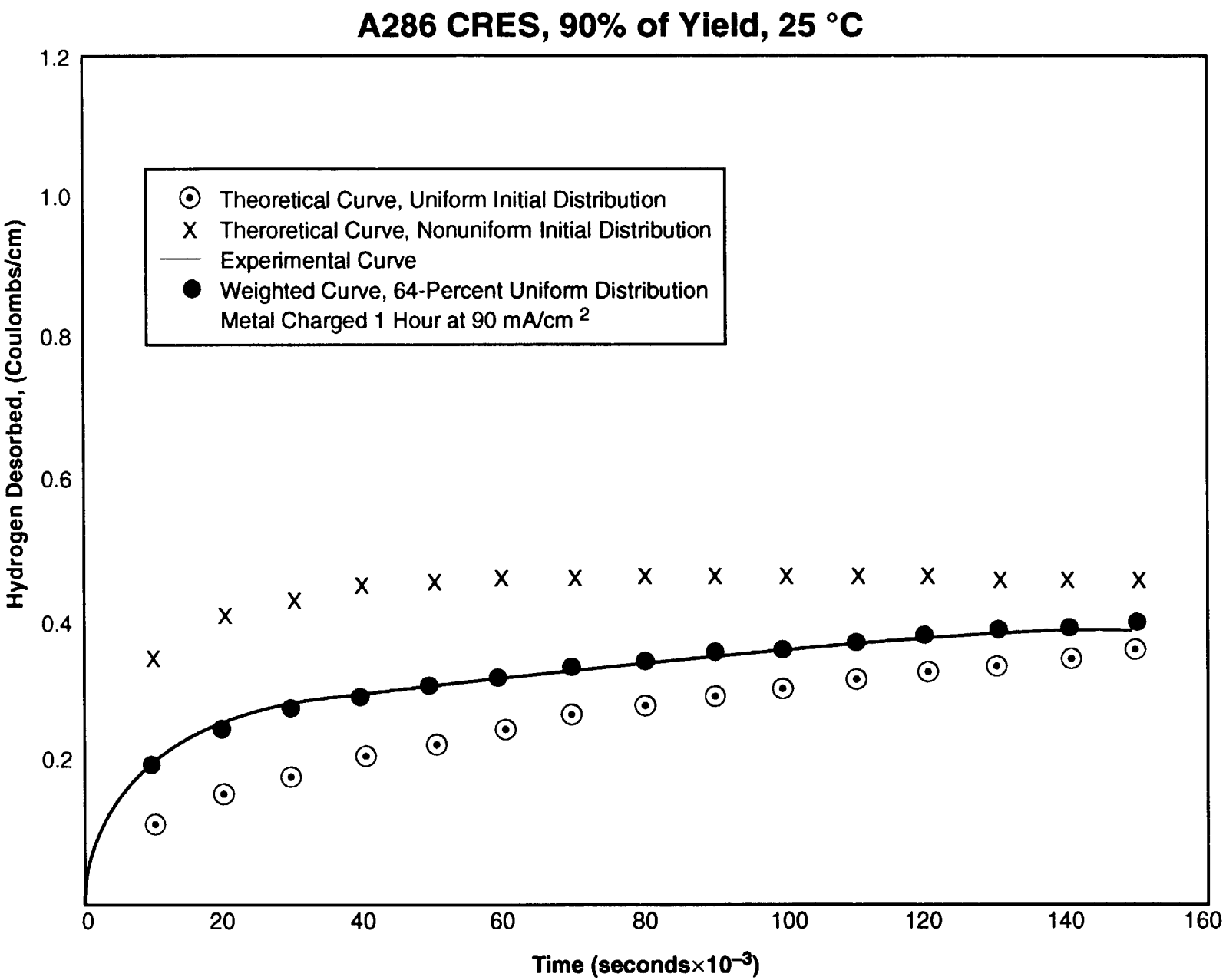

Figure 11. Hydrogen Desorption Curves for A286 CRES at 90 Percent of Yield.

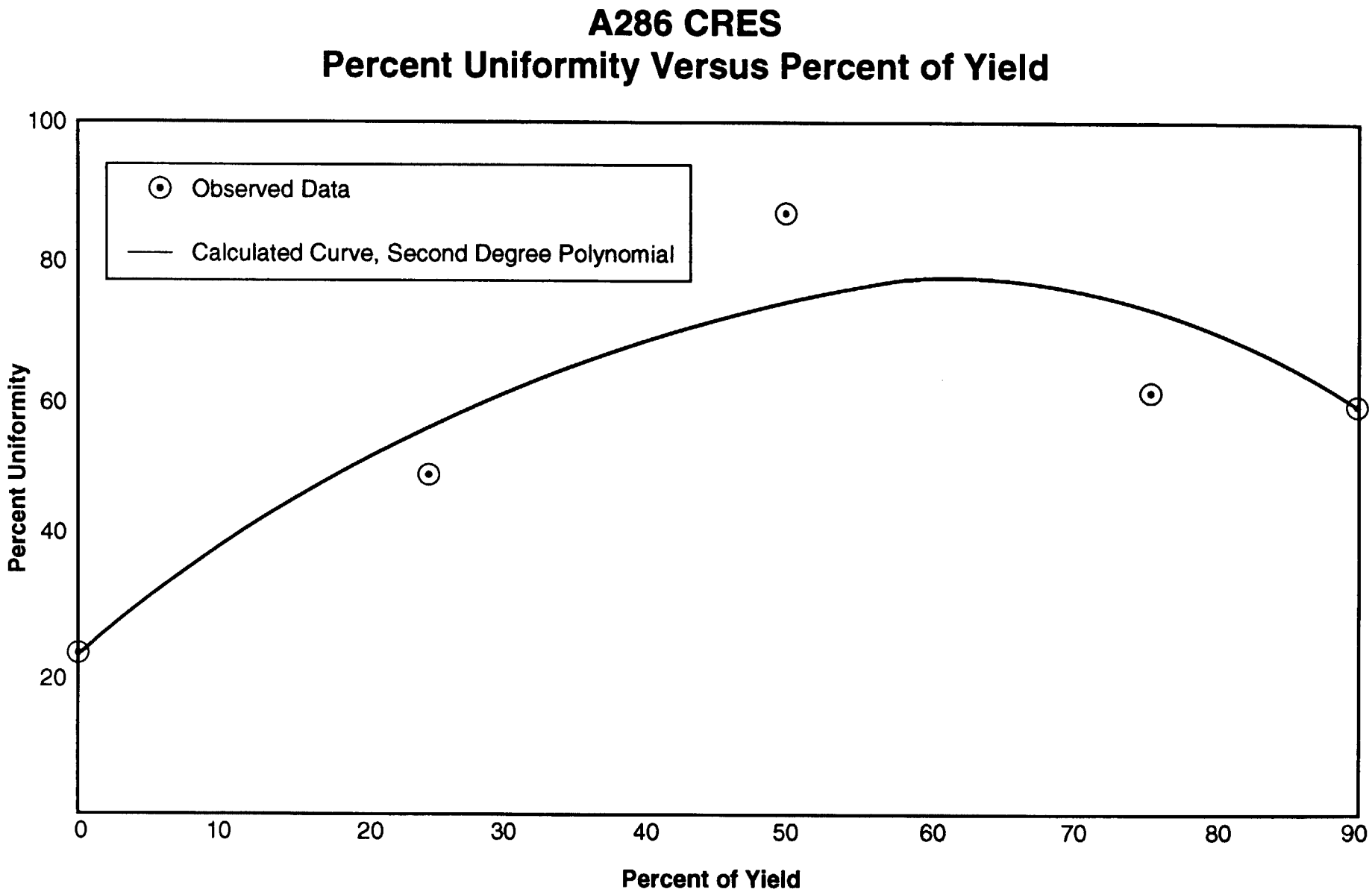

Figure 12. Least-Squares Fit of a Second-Degree Polynomial to Percent Uniformity Versus Percent Yield for A286 CRES.

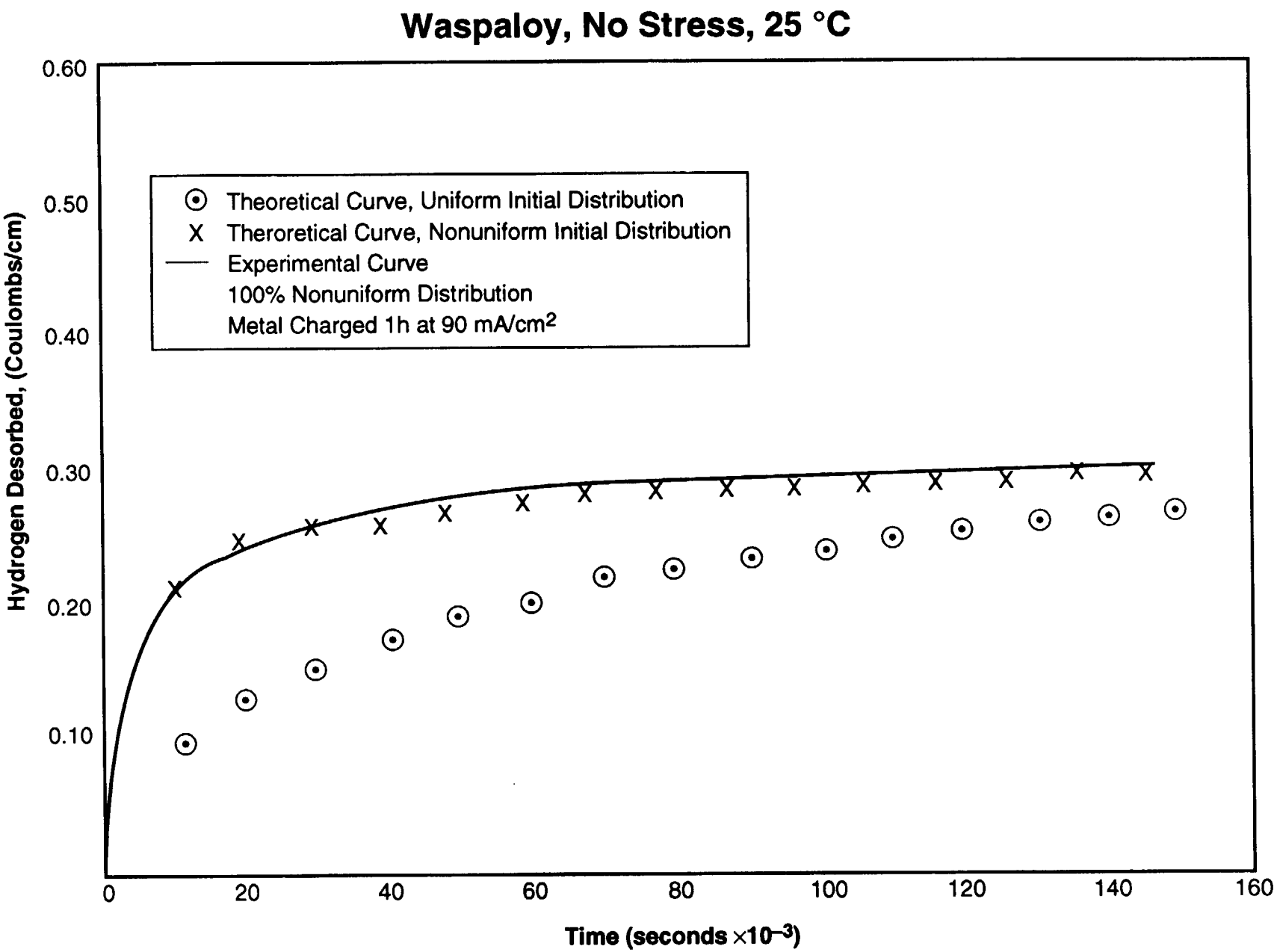

Figure 13. Hydrogen Desorption Curves for Waspaloy at Zero Stress.

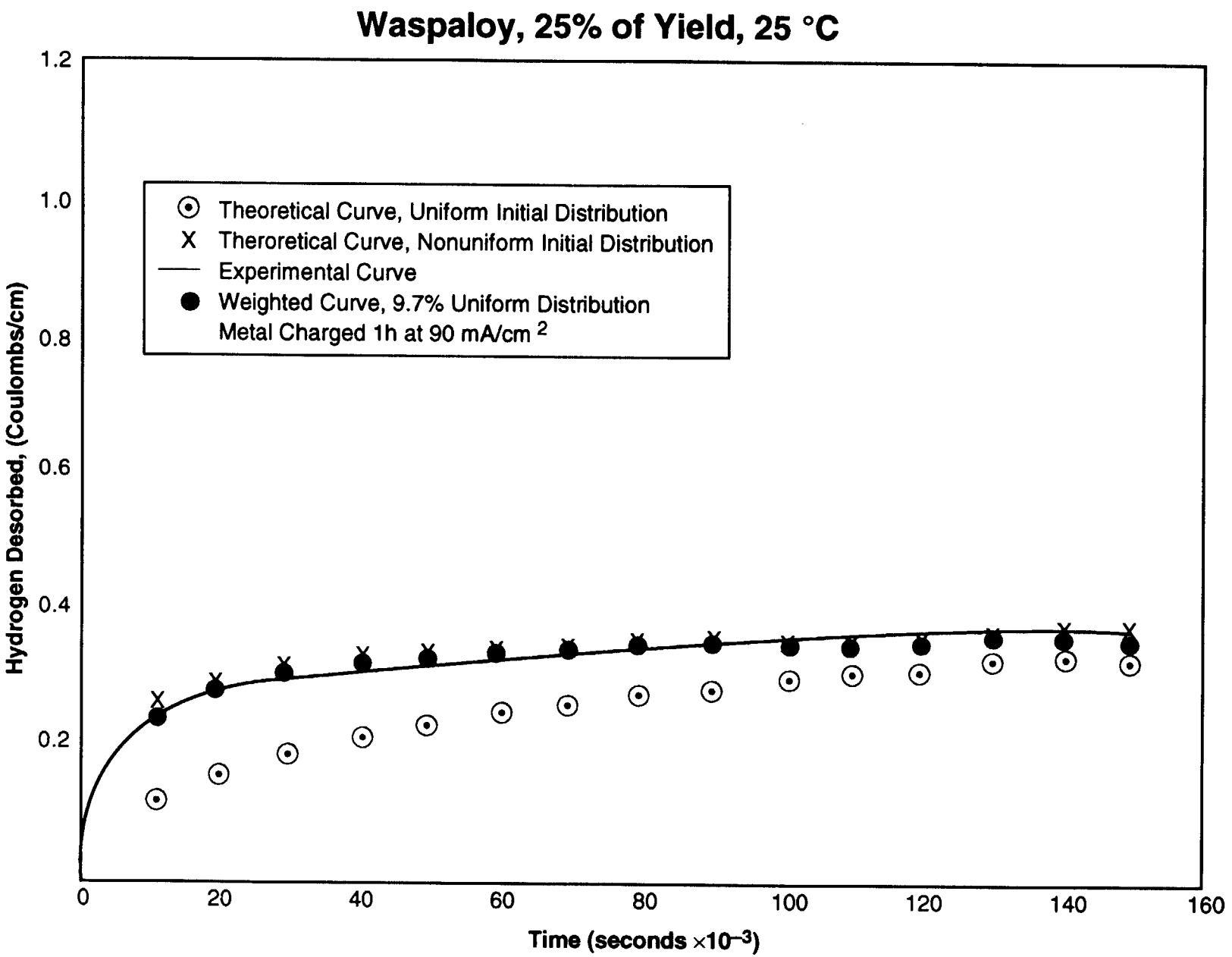

Figure 14. Hydrogen Desorption Curves for Waspaloy at 25 Percent of Yield.

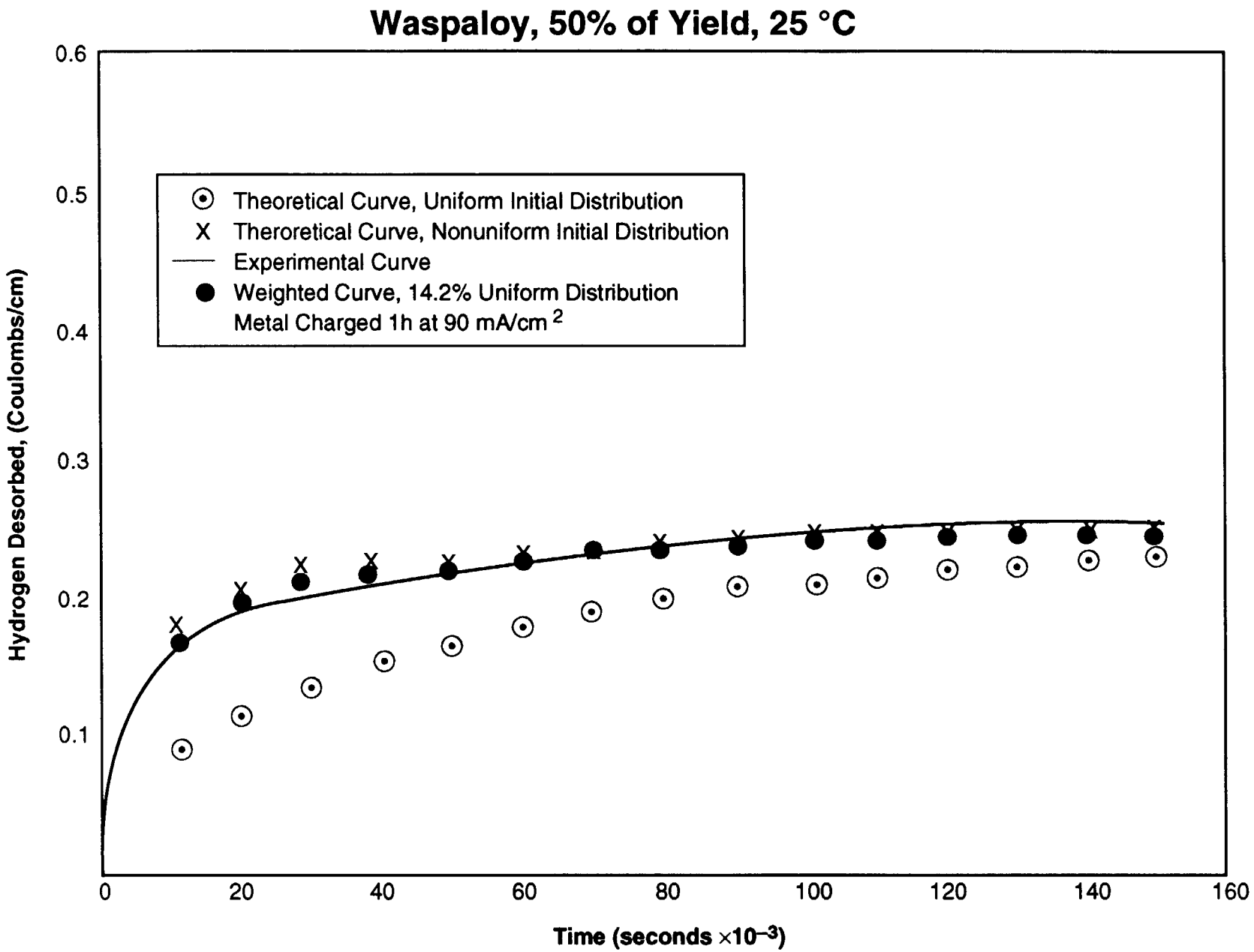

Figure 15. Hydrogen Desorption Curves for Waspaloy at 50 Percent of Yield.

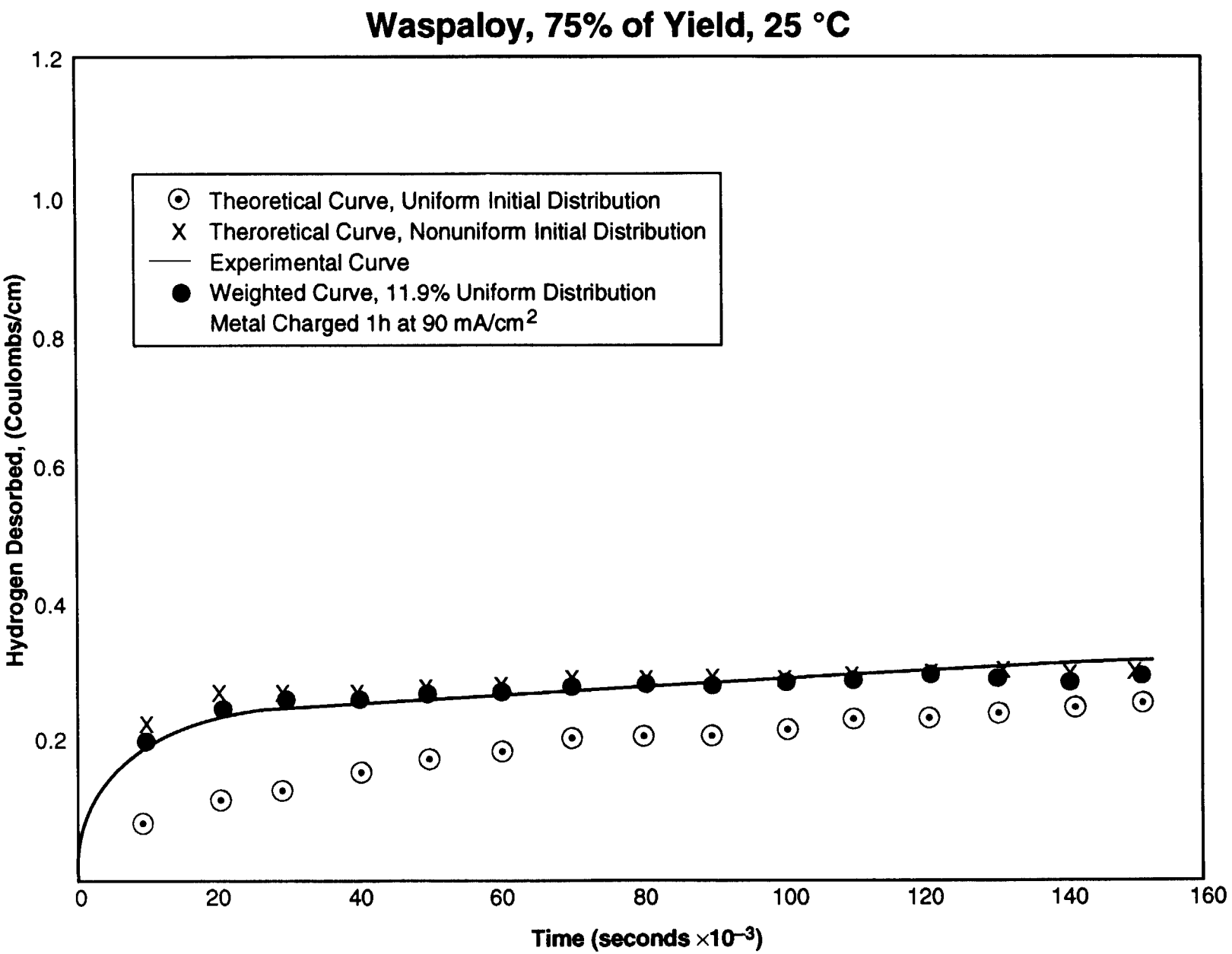

Figure 16. Hydrogen Desorption Curves for Waspaloy at 75 Percent of Yield.

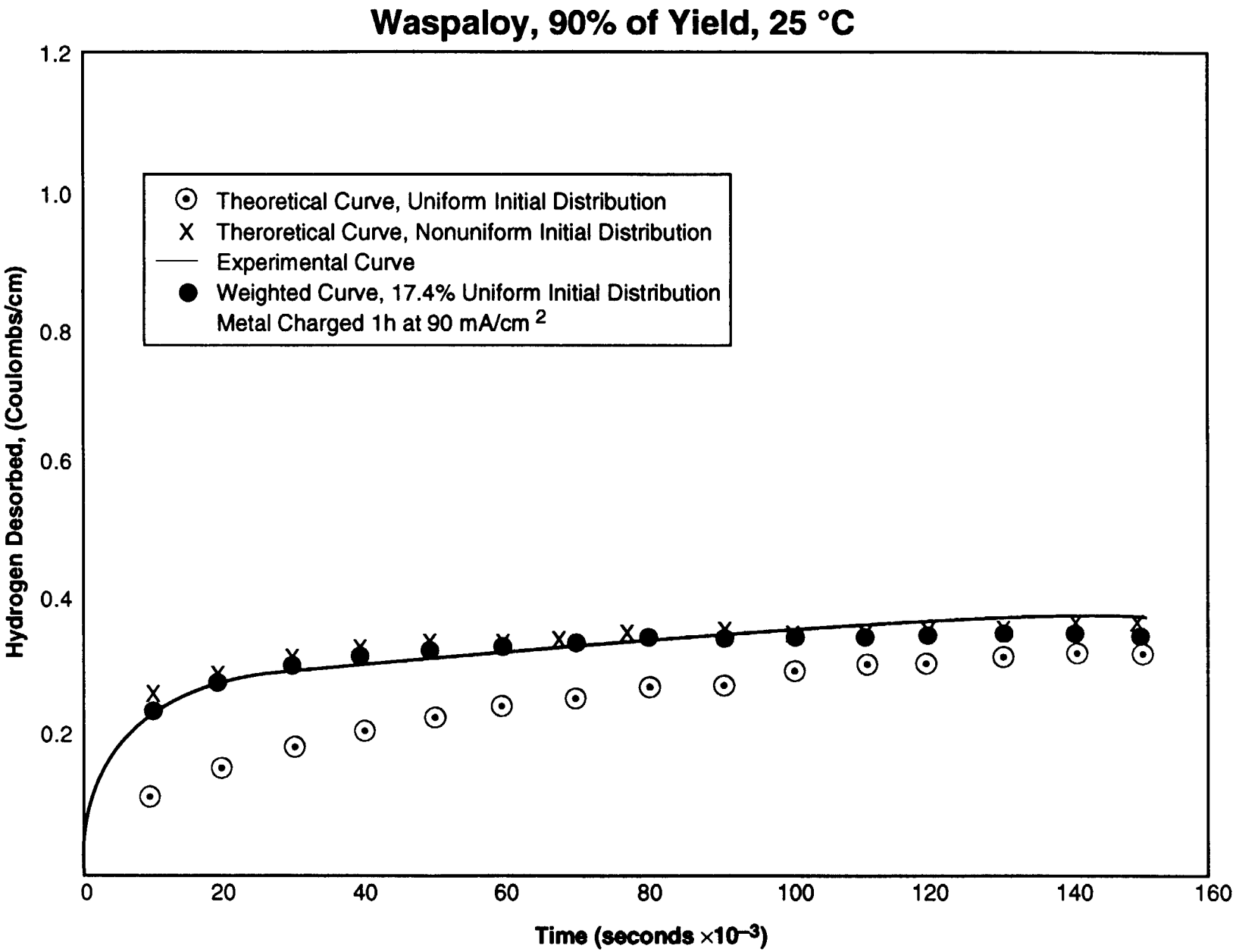

Figure 17. Hydrogen Desorption Curves for Waspaloy at 90 Percent of Yield.

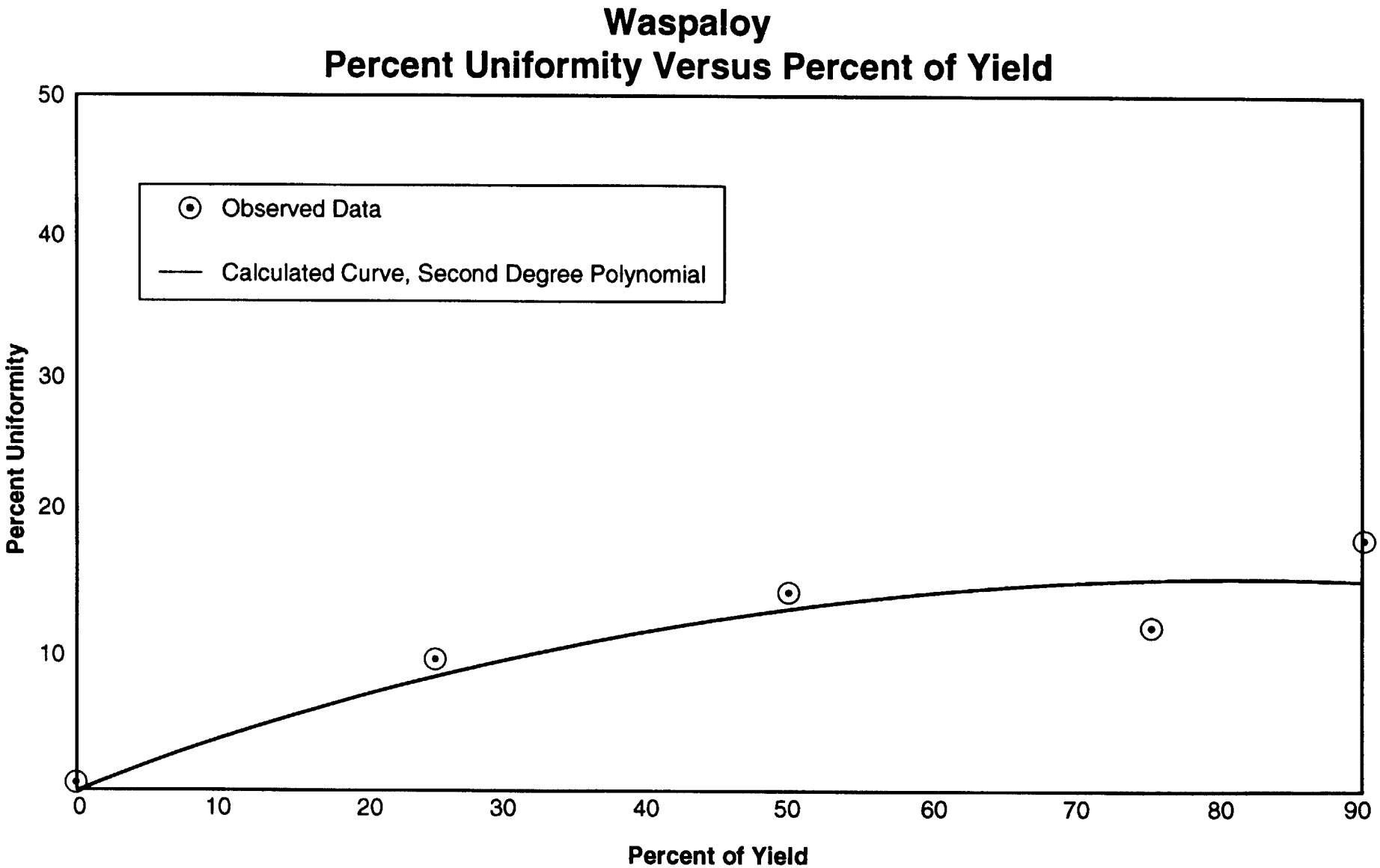

Figure 18. Least-Squares Fit of a Second-Degree Polynomial to Percent Uniformity Versus Percent Yield of Waspaloy.

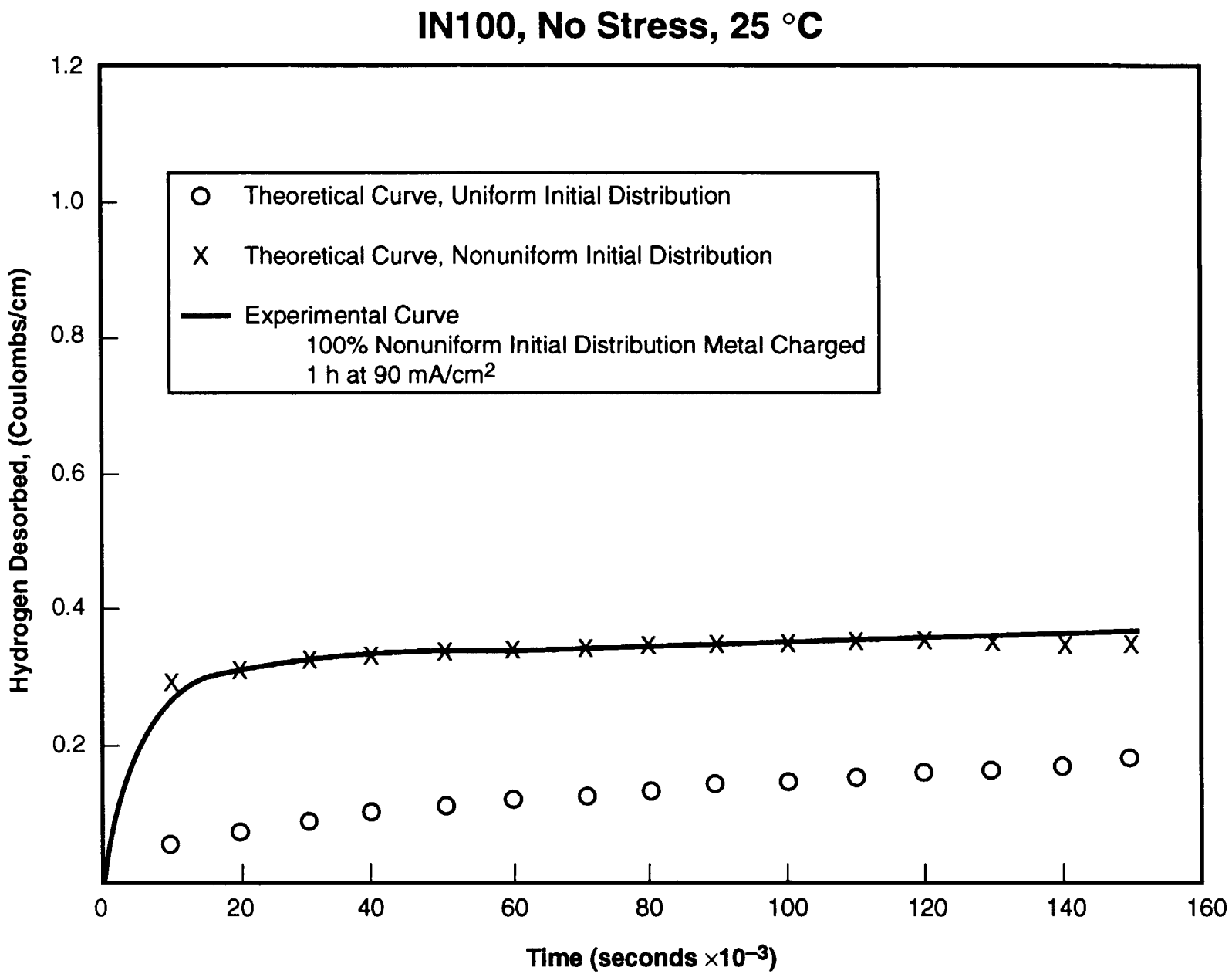

Figure 19. Hydrogen Desorption Curves for IN100 at Zero Stress.

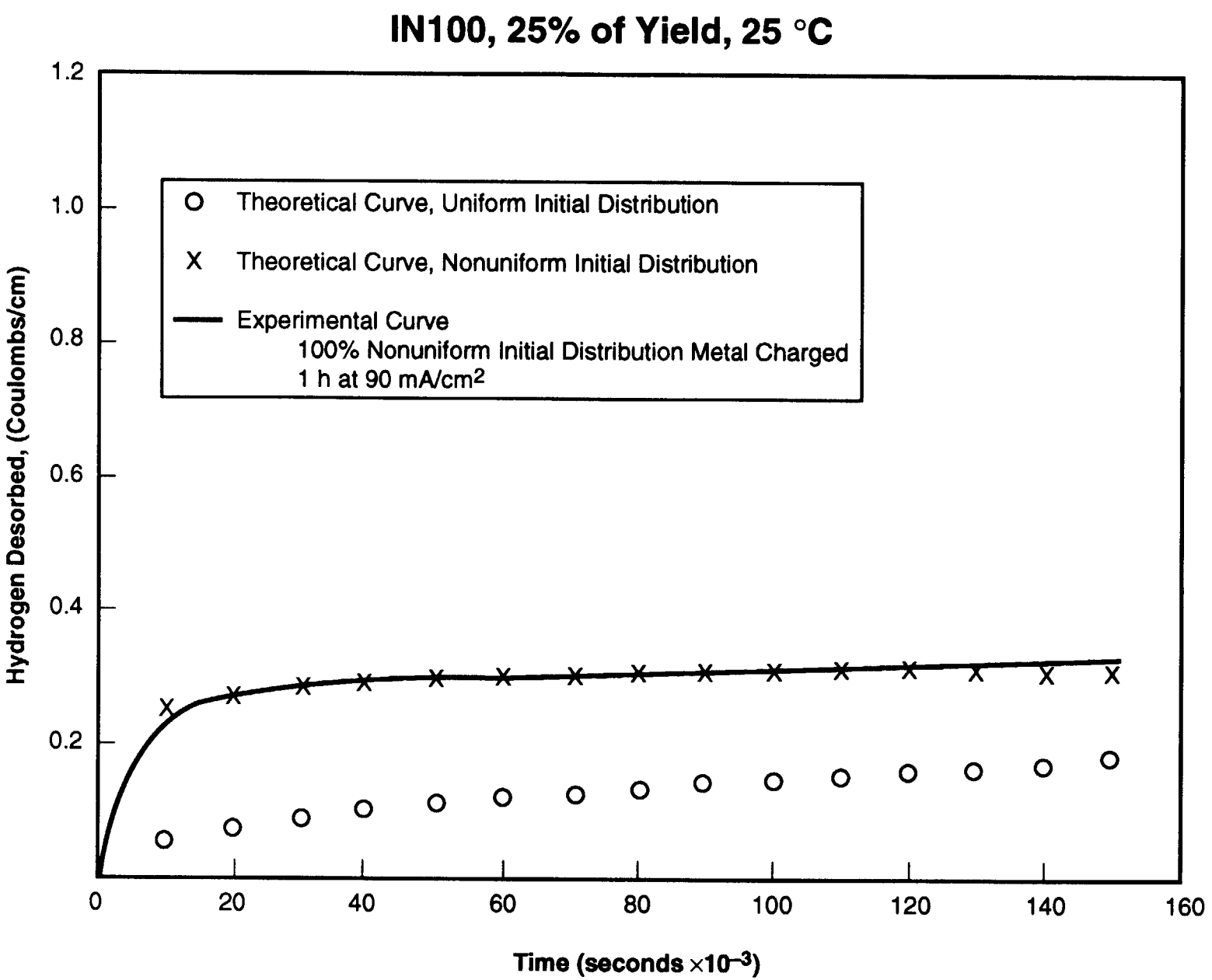

Figure 20. Hydrogen Desorption Curves for IN100 at 25 Percent of Yield.

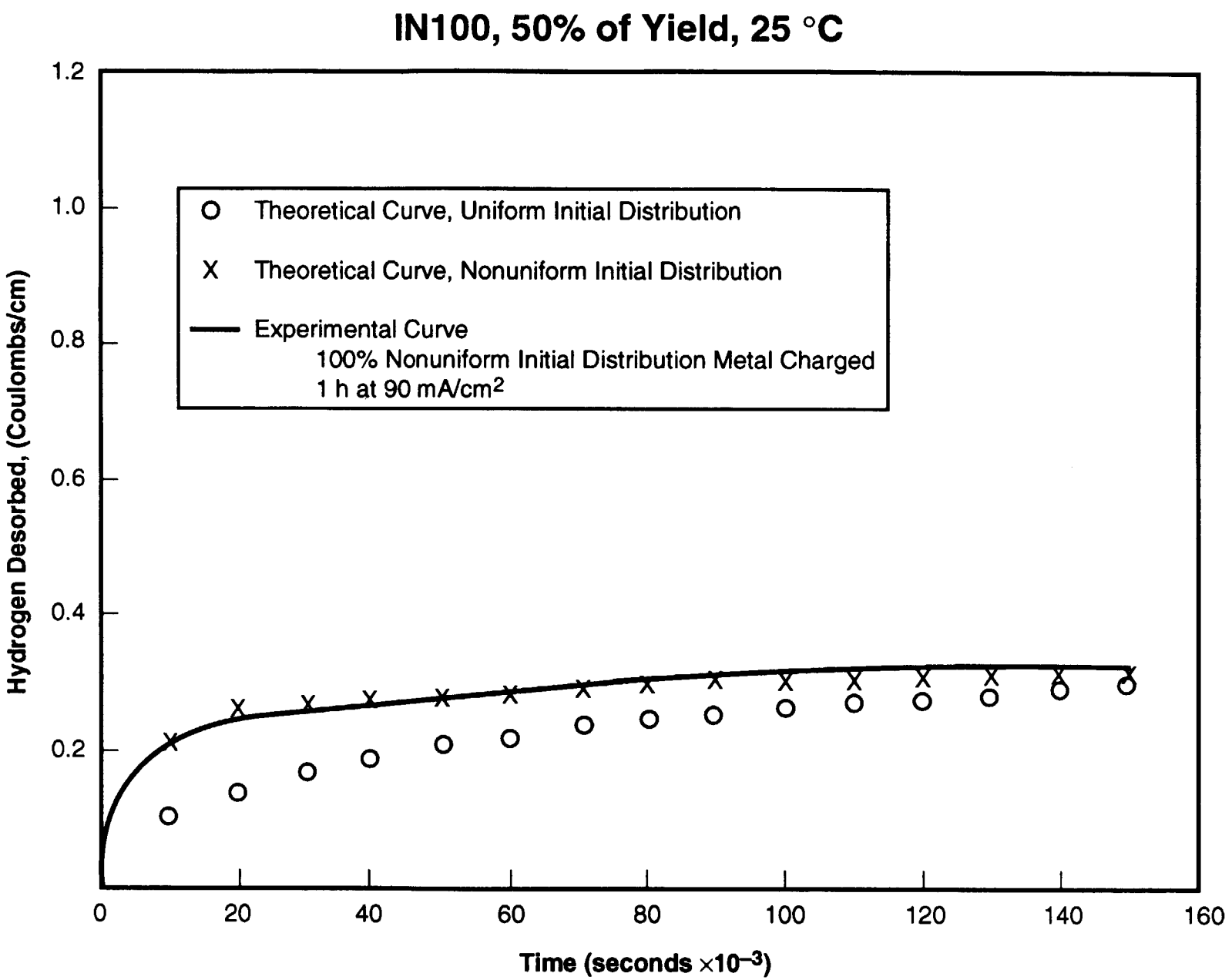

Figure 21. Hydrogen Desorption Curves for IN100 at 50 Percent of Yield.

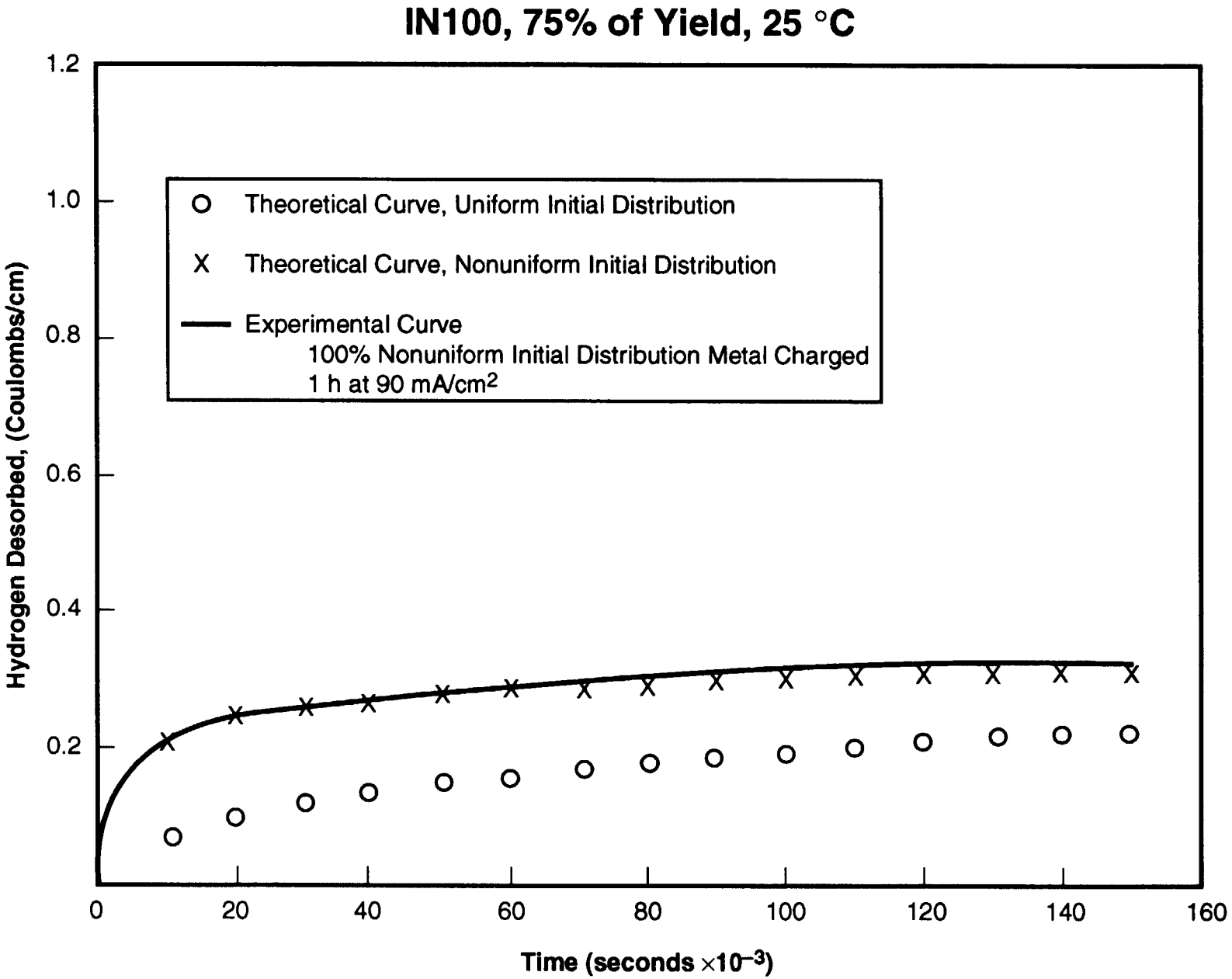

Figure 22. Hydrogen Desorption Curves for IN100 at 75 Percent of Yield.

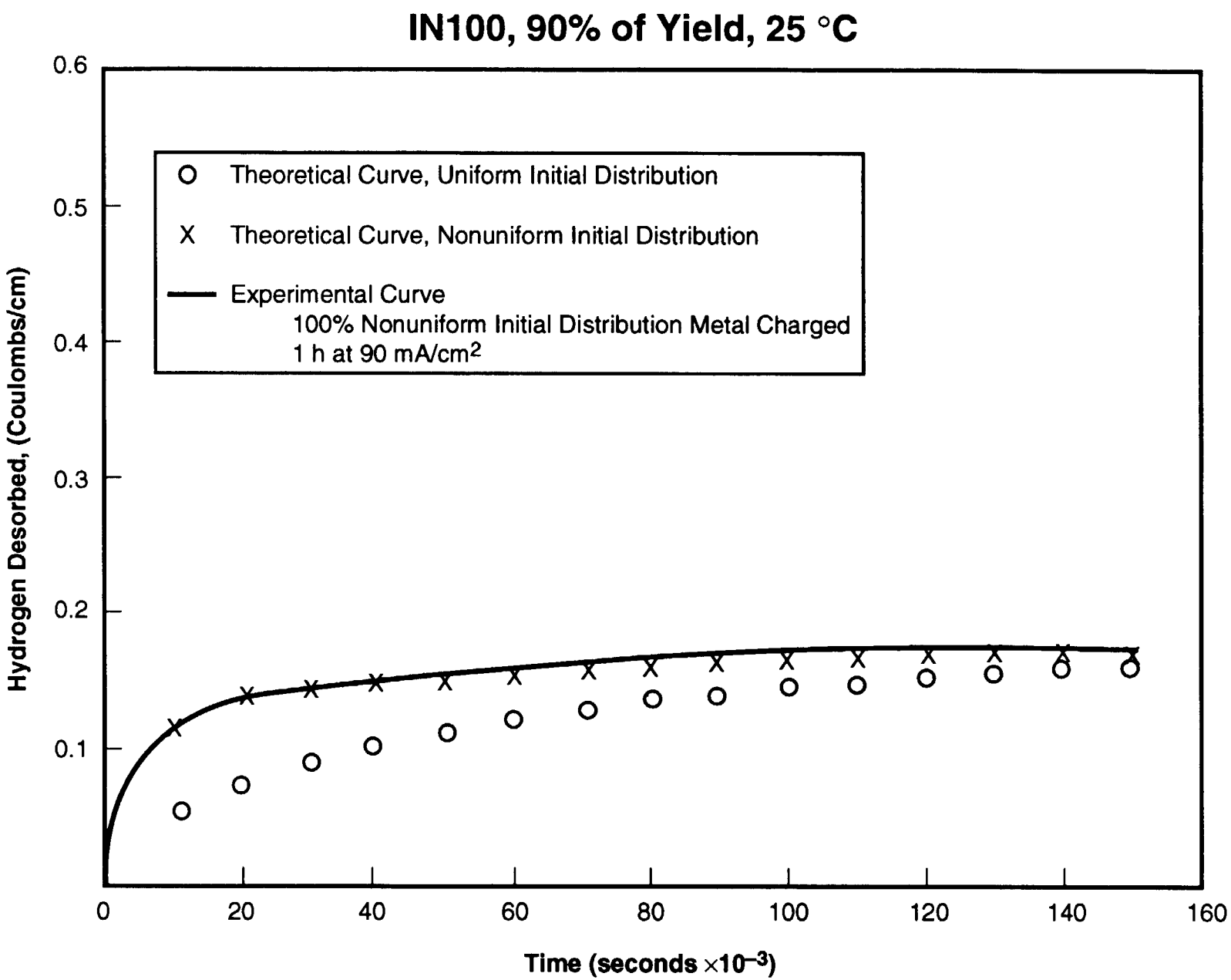

Figure 23. Hydrogen Desorption Curves for IN100 at 90 Percent of Yield.

APPROVAL

THE EFFECT OF TENSILE STRESS ON HYDROGEN DIFFUSION IN METAL ALLOYS

By M. D. Danford

The information in this report has been reviewed for technical content. Review of any information concerning Department of Defense or nuclear energy activities or programs has been made by the MSFC Security Classification Officer. This report, in its entirety, has been determined to be unclassified.

Joseph W. Montano
Chief
Corrosion Research Branch

Paul M. Munafo
Chief
Metallic Materials Division

Paul H. Schuerer
Director
Materials & Processes Laboratory

☆ U. S. GOVERNMENT PRINTING OFFICE 1992 733-060 / 80003